6. SITE 325

The Shipboard Scientific Party[1]

SITE DATA

Position: 65°02.79'S, 73°40.40'W (Antarctic Continental Rise)

Water Depth: 3748 corrected meters, echo sounding; 3745 meters, drill pipe measurement

Number of Holes: 1

Number of Cores: 10

Penetration: 718 meters

Total Length of Cored Section: 95 meters

Total Core Recovered: 34.4 meters

Percentage Core Recovered: 36%

Oldest Sediment Cored:
Depth Subbottom: 718 meters
Nature: Claystone
Age: Oligocene to early Miocene
Velocity: 3.5-4.5 km/sec

Basement: Not reached

Principal Results: Approximately 35 meters of terrigenous clay, claystone, siltstone, and sandstone were recovered from a hole drilled to 718 meters on the continental rise. The entire sequence penetrated consists of Cenozoic deposits; the oldest sediment at the bottom of the hole is Oligocene to early Miocene. The lithified detrital sediments recovered intermittently from about 400 to 700 meters probably represent sediment within and below the prominent mid-section seismic reflector at 0.37 sec subbottom which probably corresponds to the high velocity (5.25 km/sec) calcite-cemented siltstone cored at 400 meters. Analysis of a nearby sonobuoy record indicates the hole terminated about 500 meters from basaltic basement. The oldest ice-rafted debris was found in Miocene age sediment; a similar age was found for the dropstone at Site 323.

BACKGROUND AND OBJECTIVES

Background

Site 325 lies on the central portion of the continental rise northwest of the Antarctic Peninsula approximately 100 miles north of the Antarctic continental shelf (Figures 1 and 2). The continental rise slopes gently towards the northwest into the Bellingshausen Abyssal Plain; the base of the continental slope is about 80 miles to the southeast. About 230 miles to the northeast the continental rise intersects rough ridge-type topography near the Drake Passage. Water depths in the vicinity of the site are about 4000 meters, and tectonically it lies in the oceanic part of the stable Antarctic plate. Seismic profiles through the site (Figures 3 and 4) show a gently sloping continental rise underlain by less than a kilometer of sediment resting on a comparatively smooth basement. (Tracks for seismic profiles are given in Figure 5.)

The Antarctic Peninsula and its adjacent islands are the lands closest to Site 325. The geology of the Antarctic Peninsula is shown on two large-scale maps by Adie (1970) and on a small-scale map of the entire continent by Craddock (1972). The geologic history of the Antarctic Peninsula and its relation to the evolution of the Scotia Arc have been treated by Dalziel and Elliot (1973). They divide the rocks of the Scotia Arc region, including the Antarctic Peninsula, into six major units: (1) Cenozoic sedimentary and volcanic rocks, (2) late Mesozoic-Cenozoic plutons, (3) Cretaceous sedimentary and volcanic rocks, (4) upper Jurassic sedimentary and acidic volcanic rocks, (5) upper Paleozoic sedimentary rocks, and (6) metamorphic basement complexes.

No firm evidence is available from which to establish the age of the sea floor under the Southeast Pacific Basin. However, recent magnetic data (Herron and Tucholke, this volume) suggest that the crust in the vicinity of Site 325 was formed in late Oligocene-early Miocene and was generated from the Aluk Ridge spreading center which was subducted beneath the Antarctic Peninsula.

Paleocirculation patterns in the Southeast Pacific Basin are probably related to changes in paleobathymetry, although sedimentation patterns at this site near the continental shelf are more likely to be dominated by glaciation and continental erosion than to patterns of bottom circulation. However, some background information on major circulation events will serve as a regional perspective.

Site 325 lies near the western entrance to the Scotia Sea and well south of the axis of the Antarctic Circumpolar Current which flows eastward at a rate of more

[1]Charles D. Hollister, Woods Hole Oceanographic Institution, Woods Hole, Massachusetts (Co-chief scientist); Campbell Craddock, University of Wisconsin, Madison, Wisconsin (Co-chief scientist); Yury A. Bogdanov, P.P. Shirshov Institute of Oceanology, U.S.S.R. Academy of Sciences, Moscow, U.S.S.R.; N. Terence Edgar, Scripps Institution of Oceanography, La Jolla, California (Present address: U.S. Geological Survey, Reston, Virginia); Joris M. Gieskes, Scripps Institution of Oceanography, La Jolla, California; Bilal U. Haq, Woods Hole Oceanographic Institution, Woods Hole, Massachusetts; James R. Lawrence, Lamont-Doherty Geological Observatory, Columbia University, Palisades, New York; Fred Rögl, Eidg. Technische Hochschule, Zurich, Switzerland (Present address: Naturhistorisches Museum, Vienna, Austria); Hans-Joachim Schrader, Institut und Museum der Universität Kiel, Kiel, Germany; Brian E. Tucholke, Lamont-Doherty Geological Observatory, Columbia University, Palisades, New York; Walter R. Vennum, Sonoma State College, Rohnert Park, California; Fred M. Weaver, Florida State University, Tallahassee, Florida; Vasily N. Zhivago, P.P. Shirshov Institute of Oceanology, U.S.S.R. Academy of Sciences, Moscow, U.S.S.R.

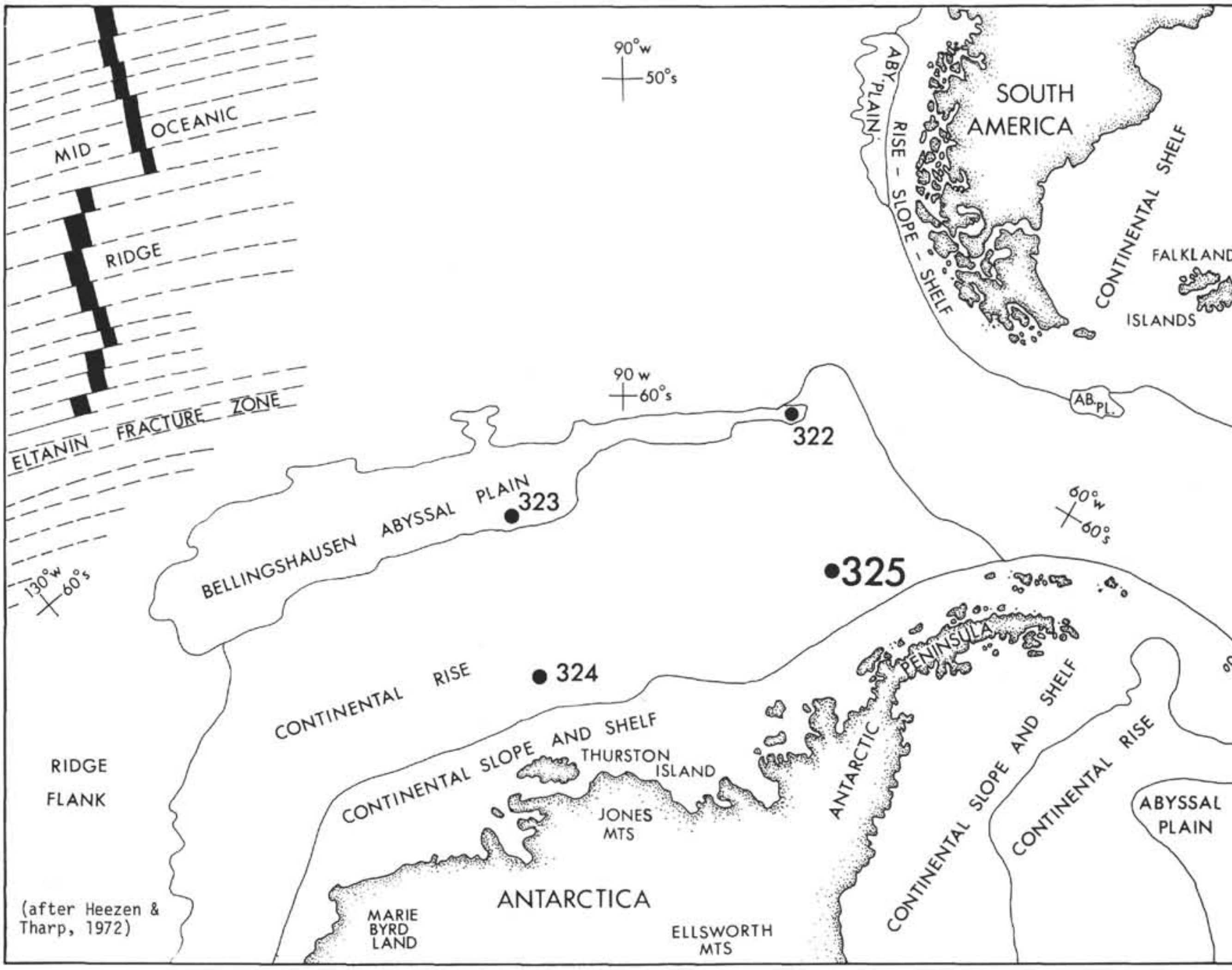

Figure 1. *Location of Site 325.*

than 200 million m³/sec (Gordon, 1967, 1972; Reid and Nowlin, 1971). Weissel and Hayes (1972) infer from magnetic anomalies that oceanic crust began forming between East Antarctica and Australia about 55 m.y.B.P., and this may be the approximate date at which the present circumpolar circulation pattern could have formed. Kennett et al. (1972) report a regional unconformity of Oligocene age in the southwestern Pacific Ocean Basin, and they attribute it to paleocirculation changes related to the separation of Australia from East Antarctica and to glacial episodes in Antarctica.

The history of continental glaciation is partially recorded in the sediments of the adjacent ocean as ice-rafted debris derived from the continent. Evidence for Tertiary glaciation in the Jones Mountains (74°S, 94°W) was first reported by Craddock et al. (1964) and later summarized by Rutford et al. (1972). LeMasurier (1972) described the volcanic history of Marie Byrd Land and suggested the existence of a West Antarctic ice sheet since the Eocene. Margolis and Kennett (1970) studied the quartz grains and foraminifers in 18 cores from the South Pacific and inferred Antarctic glaciation during much of the time since the Eocene, but with a warm episode in the Miocene. During DSDP Leg 28 glaciomarine sediments were found in holes in the Ross Sea, including beds as old as early Oligocene at one site. Because it lies further north than the rest of the continent, the Antarctic Peninsula may have had a different history of glaciation during the Cenozoic, and Site 325 is favorably located to preserve this glacial record.

Objectives

The principal objective at Site 325 was to establish the age of the oceanic crust by drilling through the sedimentary sequence into the basement. Other objectives were to determine patterns of sedimentation, water circulation, and paleobiogeography; to understand the history of Cenozoic glaciation in the Southeast Pacific Basin; to establish a biostratigraphic sequence and to reconstruct the paleooceanic environment; to obtain specimens of basement rock to determine its composition, age, and degree of alteration and paleomagnetism; to determine geochemical gradients and halmyrolysis of sediment and interstitial water.

OPERATIONS

The ship arrived in the vicinity of Site 325 at approximately 0800 hr, 19 March on a northeast course

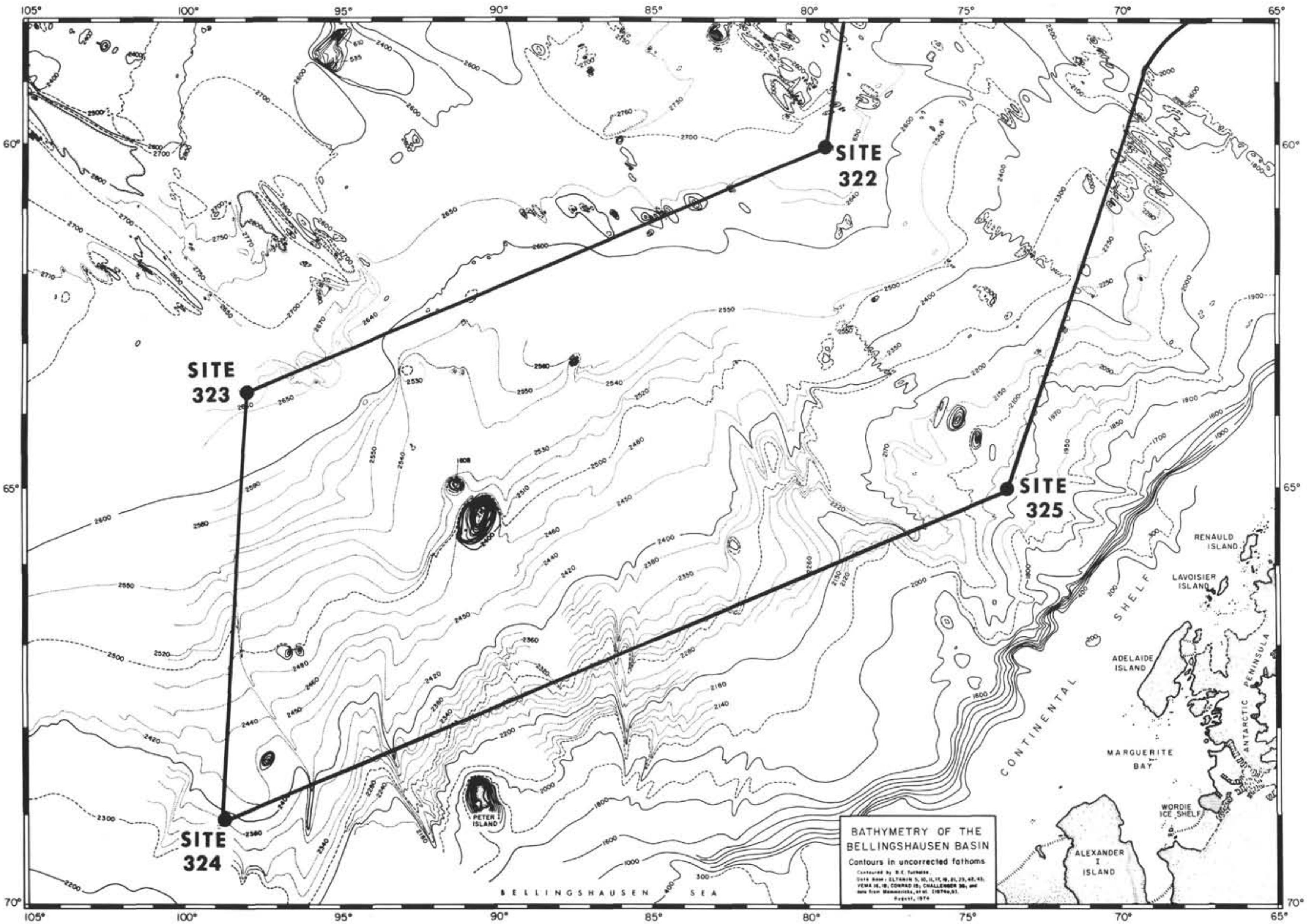

Figure 2. *Bathymetric map of the Bellingshausen region. (See also foldout in back cover.)*

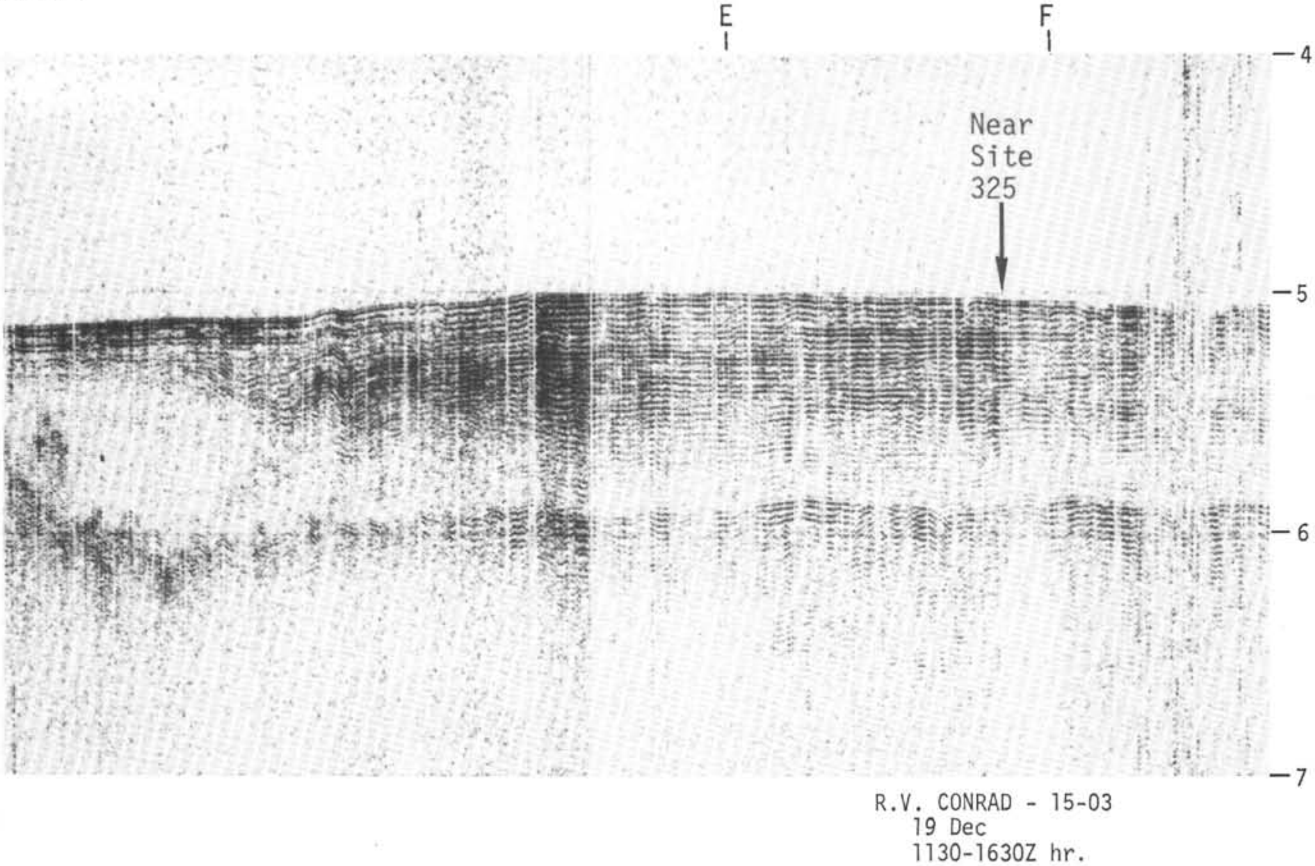

Figure 3. Conrad 15-03 *seismic profile in the vicinity of Site 325. Letters are indexed on track chart, Figure 5.*

and slowed to make a seismic profile across the *Eltanin*-43 track prior to dropping the beacon. The beacon was dropped at 1030 hr 19 March (Figure 5).

After a variety of time-consuming (2½ days) mechanical troubles combined with bad weather we began running pipe at 1500 hr on 21 March in 3748 meters (corrected echo sounding depth) at 65°02.79'S and 73°40.40'W. At this time a combination of weather and mechanical problems resulted in another 2-day delay. Finally bottom contact was made at 1200 hr at 3755 meters (from the rig floor) on 23 March.

A total of 10 cores (9.5 m each) was attempted and 34.4 meters of sediment were recovered. The hole was abandoned after Core 10 due to 20-foot swells and high (60 mph) gusty winds. Periodic hole collapse caused the bit to plug below Core 3 (186 m subbottom), and 625 barrels of mud were required to flush the hole while coring and drilling to total depth of 718 meters. Coring at Site 325 is summarized in Table 1.

LITHOLOGY

The sediment at Site 325 is composed of terrigenous clays, silts, sands, and their consolidated analogs, but the recovered sediments represent only 4.8% of the drilled sequence. The sediments are divided into two lithologic units: (1) an upper silty clay, silty claystone, and claystone unit of middle Miocene to Quaternary age, and (2) a lower, early Miocene, sandstone, siltstone, and claystone unit. The division is somewhat artificial because of the poor control and because, like Sites 322 and 323, low core recovery at mid-depth in the hole suggests the presence of significant amounts of unconsolidated sand.

Unit 1: The dominance of clay over silts and sands distinguishes this middle Miocene to Quaternary unit from the underlying unit where sandstones and siltstones predominate. The contact lies between Cores 7 and 8 (528-612 m).

Soft sticky clay extends to a depth of about 300 to 400 meters between Cores 4 and 5; Cores 5 through 7 (404-528 m) are claystones. The clays of Cores 1-4 are disturbed by coring and show no detectable primary structure. The claystones of Cores 5-7, however, are locally laminated and have common and well-developed trace fossils. Core 7 contains about 5 cm of structureless nannofossil claystone. The clays contain silt both disseminated and as discrete layers, laminae, and pods. Silt layers show no internal structure except for a few silt/clay laminae. The silt is primarily quartz, but rock fragments and heavy minerals are always found in amounts between 3% and 15%. Feldspars and opaque minerals are normally less than 5%, but the amount varies considerably. Unlike the silt beds at Site 324 most of these silts are not well sorted.

Diatoms are present in Cores 1-6; they are particularly abundant (up to 25%) in Core 4, and to a lesser extent in Core 5. In each case they are poorly preserved and fragmentary, suggesting they are largely detrital. An estimate of principal components as determined from smear slides is given in Figure 6.

Unit 2: This unit (Cores 8-10; 612.5-718 m) is predominantly early Miocene sandstone and siltstone

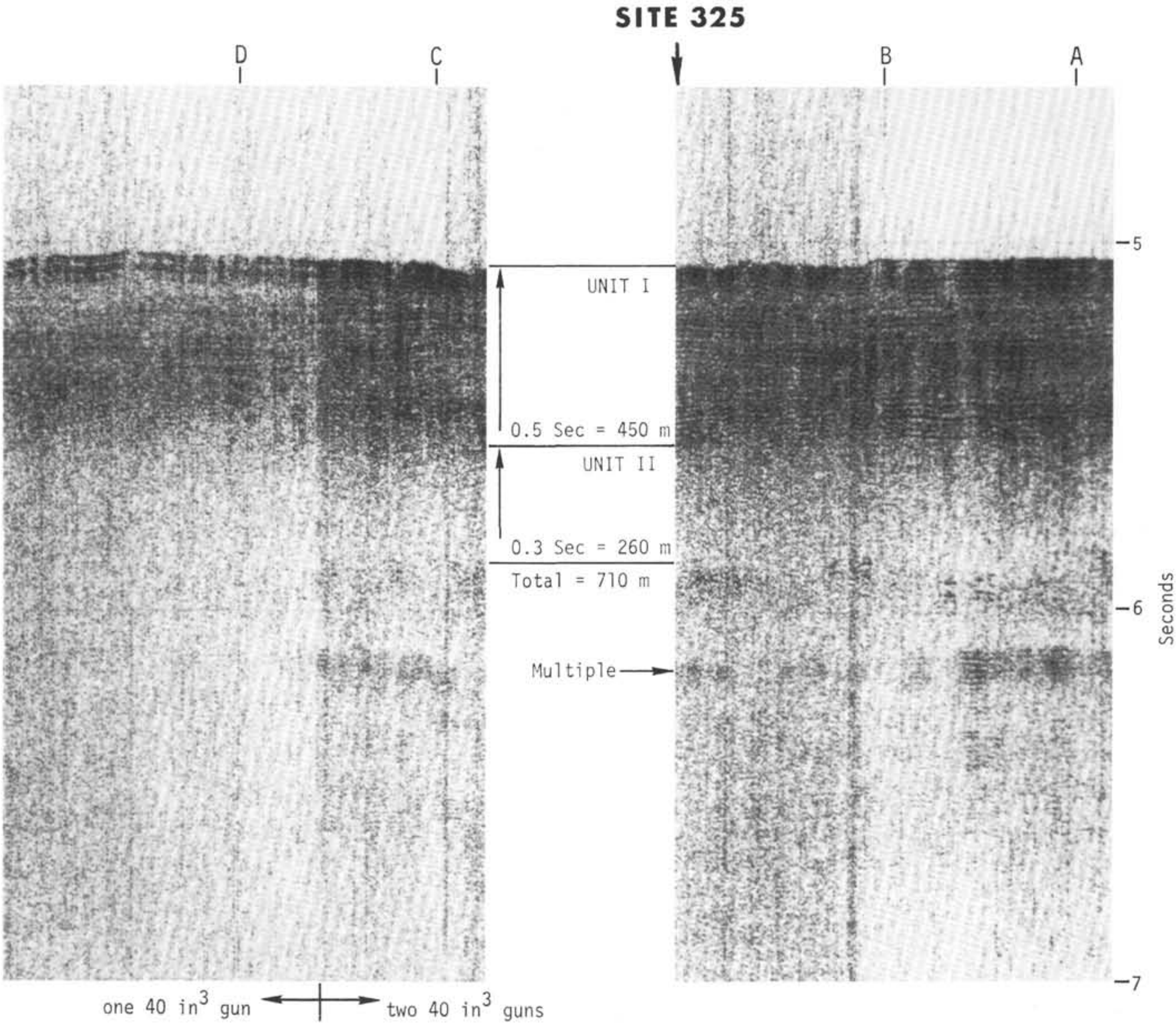

Figure 4. Glomar Challenger *seismic profile across Site 325. Acoustic units (I, II) are discussed in the text. Letters are indexed on track chart, Figure 5.*

with minor amounts of claystone. The three lithologies are interbedded throughout the unit, and sedimentary structures are clearly preserved.

The interbedded claystones are gray to olive-black and vary from massive—though extensively mottled by trace fossils—to finely laminated. They are composed dominantly of detrital clays with auxiliary quartz, feldspar, and heavy minerals in trace quantities (Figure 6). Nannofossil claystone was recovered only in Core 8, Section 2 (615 m). Lower contacts are usually gradational on siltstone, and upper contacts are marked by a sharp change to siltstone or sandstone.

The silts occur as relatively thick (approximately 10 cm) clayey beds or as thin, clean, light gray laminae in claystone. Some silt laminae occur as barely discernible partings, yet they extend in a series of parallel lines across the entire core without disturbance. In thicker layers foreset beds, interbedded clay laminae, and variations in layer thickness across the core are present. Graded bedding is uncommon and poorly developed where present. At the top of Core 8, Section 2 (642.5 m), sandy silt beds are strongly distorted due to syndepositional deformation. Deeper in the same core, faulting is clearly evident in the lithified siltstone and sandstone.

Primary structures in the sandstones encompass the spectrum created by deposition from turbidity currents: size grading, parallel laminae, foreset- and cross-bedding.

The sandstone and siltstones have a similar mineralogy, consisting dominantly of quartz, although rock fragments comprise up to 50% of the rock. Rock fragments in sandstone are generally well rounded with medium sphericity. The quartz varies from subangular to subrounded. Heavy minerals, feldspars, and detrital clays are found in most sandstones and siltstones.

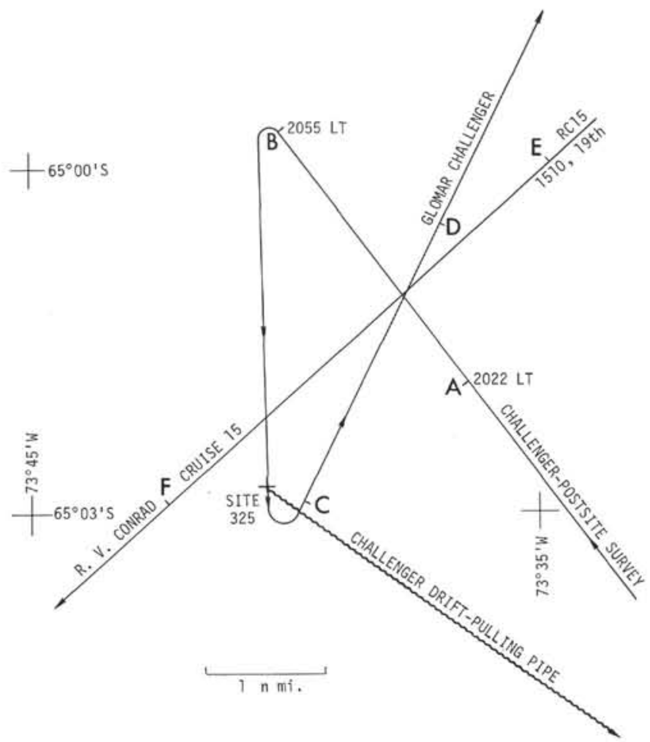

Figure 5. Glomar Challenger *and R. V.* Conrad *tracks in vicinity of Site 325. Letters on track refer to seismic profiles, Figures 3 and 4.*

Several conglomerates were found in Core 10 (708.5-718 m). They contain common to abundant clay clasts which in some cases are preferentially oriented parallel to the bedding. The matrix is usually siliceous clay, but one sample in Core 10, Section 3 is cemented with authigenic carbonate.

Authigenic cementation of sediments by silica and calcite is common below Core 4. Recognizable tests of diatoms and radiolarians decrease in abundance below this level, and dissolution and reprecipitation of the biogenic silica apparently has caused the observed cementation. Nannoplankton were found in significant quantities only in the deeper part of the hole (Cores 7 and 8); however, dissolution and precipitation of biogenic calcite apparently does not account for the calcite cementation inasmuch as carbon isotope compositions are different in the two carbonates (see Anderson and Lawrence, this volume).

Interpretation

The lithology at this site is, in general, very similar to that of Site 324; both sites are on the continental rise of the Bellingshausen coast.

A qualitative estimate of the amount of ice-rafted material as well as the percent of quartz silt in the clays, the average number of silt laminae per meter of core, and the percentage abundance of diatoms is tabulated in Figure 10 (Summary and Conclusions section).

The quartz-in-clay percentage and the number of silt layers per meter are inversely related. Every decrease in the quartz content of the clay is matched by a corresponding increase in number of silt layers. Thus the quantity of quartz supplied to the area has apparently been fairly constant, and the variations in the number of layers to quartz-in-clay content relate directly to the distributing process.

However a significant increase in the amount of quartz-in-clay from Core 2 to Core 3 is matched by an

TABLE 1
Coring Summary, Site 325

Core	Cored Interval		Cored (m)	Recovered		Lithology	Age
	Total Depth (m)	Subbottom Depth (m)		(m)	(%)		
1	3789.0-3798.5	34.0-43.5	9.5	6.1	59	Clay and silty clay	Pliocene
2	3922.0-3931.6	167.0-176.5	9.5	2.6	27	Igneous and metamorphic gravel and diatom-bearing clay	Pliocene
3	3931.5-3941.0	176.5-186.0	9.5	5.0	52	Sand, silt, and clay	Pliocene
4	4045.5-4055.0	290.5-300.0	9.5	3.4	36	Claystone and fine gravel	Pliocene
5	4159.5-4169.0	404.5-414.0	9.5	2.0	21	Claystone and siltstone	Pliocene
6	4235.5-4245.0	480.5-490.0	9.5	0.3	3	Silty claystone	Late Miocene
7	4273.5-4283.0	518.5-528.0	9.5	2.2	23	Claystone and nanno-fossil chalk	Early Miocene
8	4368.5-4378.0	612.5-622.0	9.5	4.4	47	Claystone with chalk and sandstone beds	Early Miocene
9	4397.0-4406.5	641.0-650.5	9.5	3.6	38	Sandstone, siltstone, and claystone	Early Miocene
10	4463.5-4473.0	708.5-718.0	9.5	4.7	49	Sandstone, claystone, and conglomerate	Early Miocene
Total	4473.0	718.0	95	34.4	36		

Recovery of total sequence penetrated = 4.8%

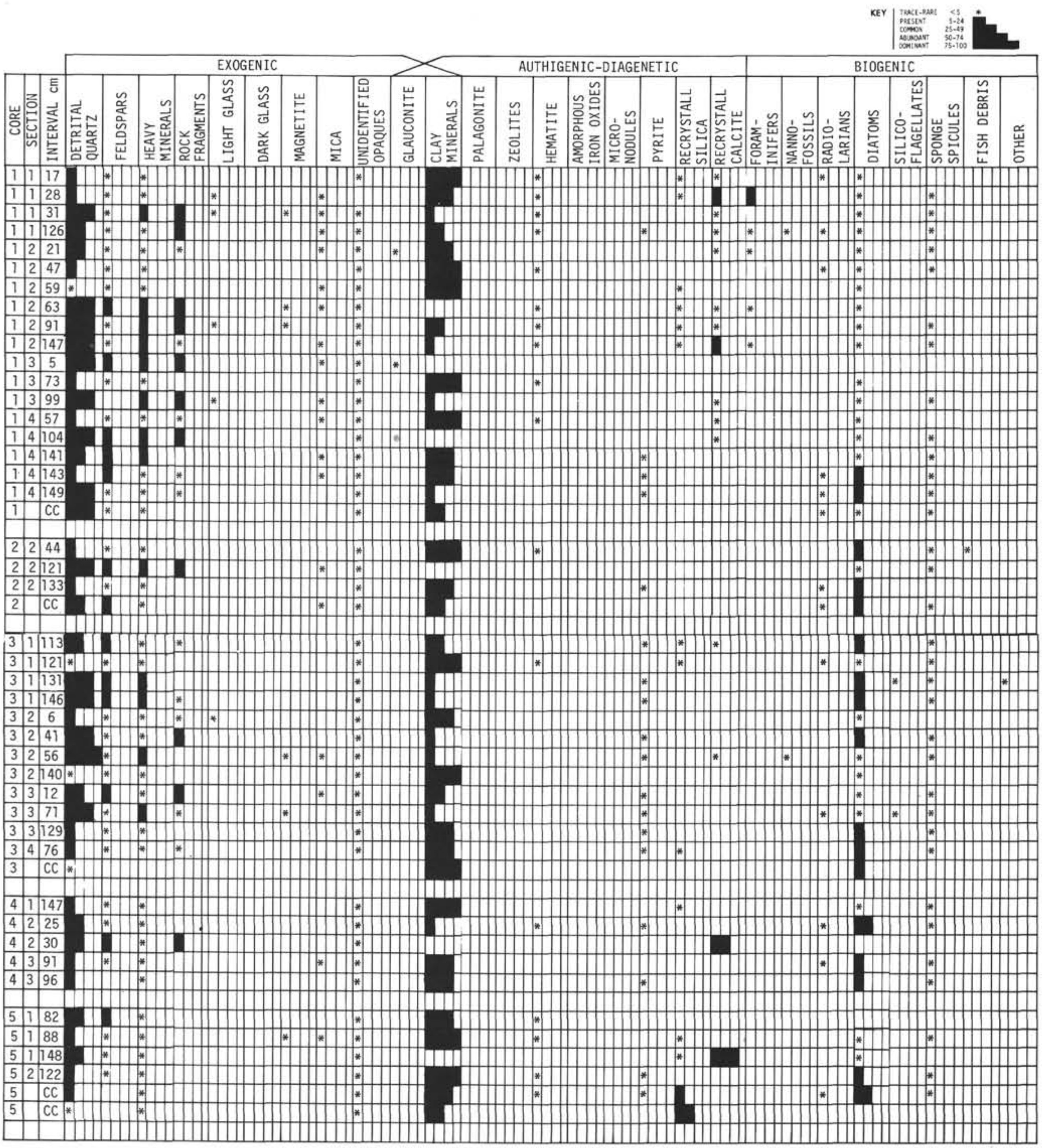

Figure 6. *Estimate of principal components from smear slides, Site 325.*

increase in the amounts of ice-rafted debris thus suggesting that ice rafting may be the sole source of the silt. The reduction in ice-rafted debris above this zone may be due to changes in glacial activity and ice cover which could be related to the formation of the bottom water that deposited the abundant silt laminae or contourites (Hollister and Heezen, 1972).

Diatoms increase in Cores 4 and 5, but they are missing from all cores below Core 6 (480 m). The fluctuations in diatom abundance seem to be independent of the other graphed variables except for a vague inverse relationship to ice-rafted material.

Sedimentation Processes

Cores recovered at this site show very little evidence of bottom current activity. Cores 1 and 2 contain disturbed silt beds which are similar to those at Site 324, but which normally have gradational upper contacts. These beds also show poor to very poor sorting and only rarely are very well sorted beds observed. The

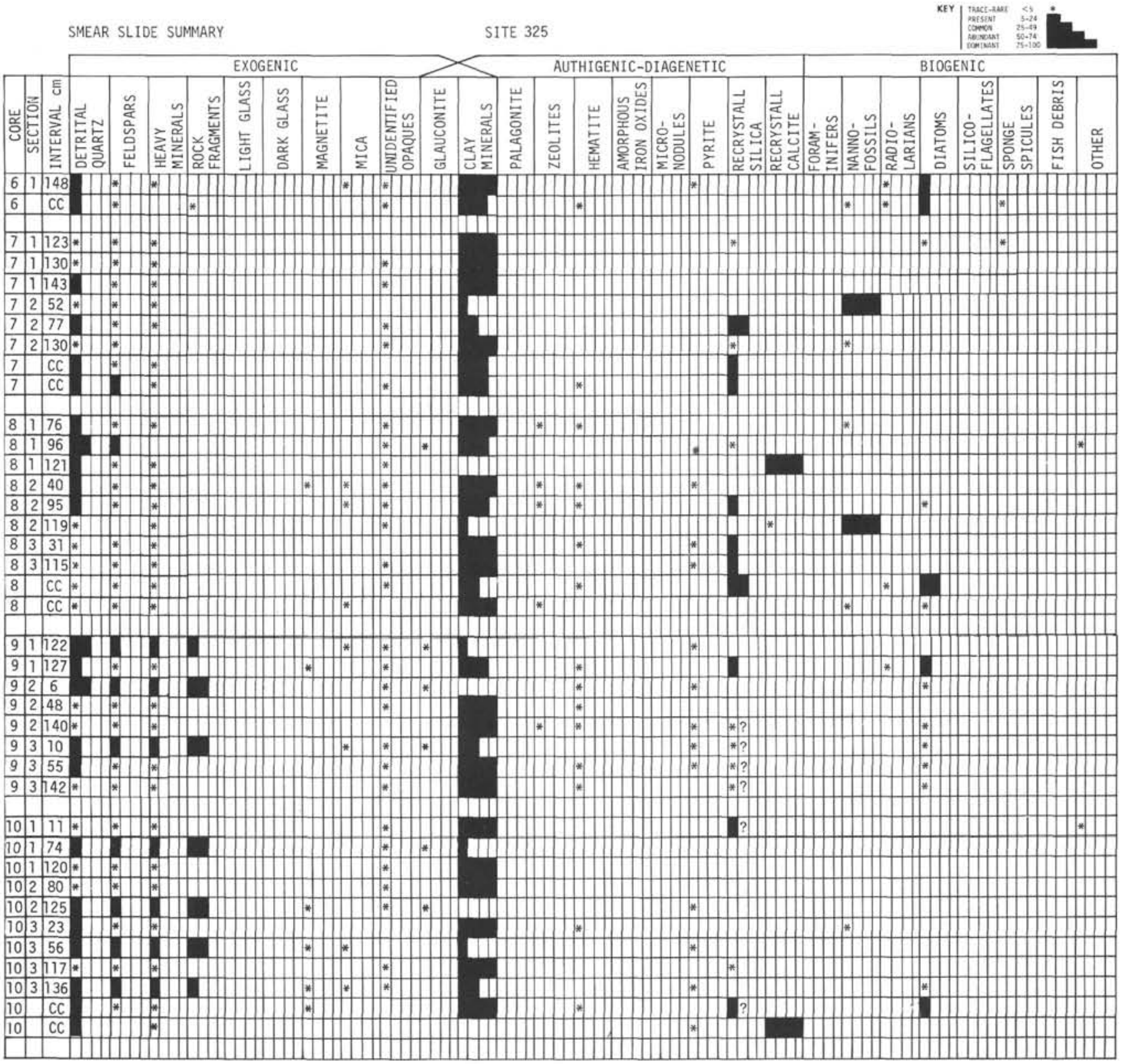

Figure 6. *(Continued).*

deeper cores contain sedimentary structures diagnostic of turbidites with little indication of current reworking. A few samples analyzed for grain size and from Pliocene sediments show the good sorting and sigmoid curves that we associate with a clayey contourite (see Tucholke, Hollister, Weaver, and Vennum, this volume). However, it is apparent that turbidite deposition has dominated the area since the early Miocene.

Site 325 was drilled in the central continental rise near the upper boundary of braided channel development (see Schroeder, this volume). All the cores recovered contain some record of turbidity current activity, and there is a general upward progression in the hole from deposition of very coarse to fine detritus. Tucholke and Houtz (this volume) have correlated this with changes in the depositional style as the area evolved from an abyssal plain to a central continental rise.

Grain size analyses from this site (see Tucholke, Hollister, Weaver, and Vennum, this volume) show a series of curves that may be grouped into: (1) sediment that is influenced by ice rafting (2) sediment that may be deposited by turbidity currents, and (3) possible clay contourite material deposited from nepheloid layers. These latter curves have the sigmoid shape of probable clayey contourites at Site 324, but they also have a few percent more silt and are less well sorted; thus they may reflect influence on both turbidite and contourite deposition.

One of the claystone conglomerates was sampled for detailed grain size; however, its fine median size (8ϕ) indicates destruction of clay clasts during the analysis.

A variety of depositional and postdepositional structures is well preserved in Cores 8 through 10. Three conglomerates were observed; all were in Core 10. They contain angular to rounded clay clasts of a variety of colors and lithologies. Clast plasticity at the time of deposition is often indicated by deformation and interpenetrative structure. For such plastic clasts to have maintained their integrity during transportation, they must have been derived close to the depositional site. Thus they may indicate nearby slumping or may have been ripped up from the adjacent sea floor by a major flow.

Sharp, irregular basal contacts of turbidites are common, and the irregularity results both from erosion and loading. Intervals of the Bouma sequence (Bouma, 1962) are commonly observed, in some places showing almost a complete sequence.

Syndepositional and postdepositional structures are common. The fluidity of sandy silt turbidites has resulted in flow and disruption of initially level bedding. Faulting of lithified sediment was also observed.

GEOCHEMISTRY

The upper part of this section is dominated by a detrital suite of minerals, and only below 630 meters does an illite/smectite of authigenic origin become a dominant clay fraction component. Slightly increased Mg/Al ratios of these sediments (Donnelly and Wallace, this volume) may reflect this. Of interest here is the essentially zero concentration of magnesium in the interstitial waters in this sediment section.

In general, the mineralogies of the sediments of Site 325 is very similar to Site 322, with volcanic components becoming of importance in the lowermost sections.

Oxygen isotope studies on sediments of Sites 322, 323, and 325 suggest a predominant terrigenous detrital suite of silicates (Anderson and Lawrence, this volume). Slight enrichments in δO^{18} in the basal brown claystones (>638 m) at Site 323 suggest the possibility of low temperature alteration of volcanic debris. This interpretation is strengthened by the similarity in δO^{18} in the bulk silicate (Anderson and Lawrence, this volume) and the <1 μm clay and quartz fraction (Eslinger and Savin, this volume).

Gorbunova (this volume) interprets the high degree of crystallinity of the montmorillonites below 638 meters at Site 323 in terms of interaction of fluids of hydrothermal origin with these sediments, without a specific knowledge of precursors.

Interstitial water analyses (Site 325) suggest that a source for calcium and sink for magnesium are located in the upper sediments. High sedimentation rates in the upper section allow the lower sediments to become essentially a closed system. As a result, complete depletion of magnesium occurs in the lower sections that are characterized by larger volcanic contributions (Perry et al., Gorbunova, both this volume). Dissolved calcium shows very large increases, probably due to alteration of underlying basalts(?).

In general, the data suggest that postdepositional alteration reactions are important in these sediments. Changes in δO^{18} of the interstitial fluids indicate that alteration of volcanic debris of basalt is of importance. The alteration reactions involve the uptake of magnesium (montmorillonite) and of potassium (zeolites, K-feldspar?) from the interstitial waters and the release of Ca (from plagioclase and augite). Alkalinity decreases toward the deeper parts of the hole, as does the total CO_2 content. This can best be understood in terms of the precipitation of calcium carbonate. Indeed, authigenic calcite shows very low C^{13}/C^{12} ratios (δC^{13} as low as -20‰, Anderson and Lawrence, this volume), indicating a primarily biogenic source of carbon dioxide (due to sulfate reduction) and involving a small amount of the calcium released during the alteration reactions described above. The alteration reactions also will involve changes in alkalinity, but little can be said about quantitative amounts involved, since we lack precise information on the reaction mechanisms.

PHYSICAL PROPERTIES

Only nondiatomaceous sediments were sampled for physical-properties measurements at Site 325, and most of them were clays or claystones. The sediments at this site consist of interbedded sands, silts, and clays and their consolidated analogs. However, there are common occurrences of siliceous cementation and, unlike the other sites, of well-developed calcite cementation. Unfortunately, cores were recovered from widely spaced intervals, so that the distribution of these materials and variations in physical properties are only very broadly defined. The physical properties data are summarized in Table 2 and Figure 7.

Aside from the shallowest measurements at 35-40 meters, water contents and porosities are fairly constant at 25% to 35% and 45% to 55%, respectively, down to 500 meters. The shallow clay samples have 35% to 45% water content and 60% to 70% porosity. A calcite-cemented siltstone at 406 meters exhibits greatly decreased water content (5.3%) and porosity (13%), and in deeper samples calcite cementation undoubtedly has reduced both water content and porosity.

Water content drops to about 15% to 20% and porosity to about 40% below 500 meters. Smear-slide examination of sediment in Cores 7 through 10 shows that minor recrystallized silica is common over this interval, and the slight silica cementation has probably contributed to the reduction in void space.

Saturated bulk density of the sediment also increases slightly at these depths to values of 1.94-1.97 g/cm^3. Between 100 and 500 meters densities are quite variable, ranging from 1.7 to 2.0 g/cm^3, with a median of about 1.8 g/cm^3. In the poorly consolidated sediment at 35 to 40 meters the densities are less than 1.75 g/cm^3. The downhole saturated-bulk-density values are virtually a mirror image of variations in water content and porosity (Figure 7).

Exclusive of diagenetically cemented sediments, values of sonic velocity show a general increase downhole. The calcite-cemented sediments in this hole have exceptionally high velocities; the siltstone at 406 meters was measured at 5.27 km/sec, and calcite-cemented conglomerate and sandstone at 713 meters have velocities of 3.56 and 3.49 km/sec, respectively. The claystone sample from 519.5 meters appears to owe its high velocity (2.37 km/sec) to slight siliceous cementation.

TABLE 2
Summary of Physical Properties, Site 325

Sample (Interval in cm)	Estimated Depth (m)	Velocity (km/sec) ∥ Beds	Velocity (km/sec) ⊥ Beds	GRAPE Special 2-Min Count Sat. Bulk Density (g/cc) ∥ Beds	GRAPE Special 2-Min Count Sat. Bulk Density (g/cc) ⊥ Beds	Sat. Bulk Density (g/cc)[a]	Wet Water Content (%)	Grain Density (g/cc)[a]	Porosity (%)[a]	Impedance (g/cm² sec) × 10⁵	Lithology Remarks
1-1, 134-135	35.34					1.56[a]	44	2.84[a]	69[a]		Disturbed silty clay
1-3, 135-150	38.35					1.72[a]	36	2.84[a]	61[a]		Disturbed silty clay
2-1, 140-141	168.40					1.86[a]	27	2.75[a]	51[a]		Disturbed silty clay
3-2, 70-71	178.70					2.00[a]	24	2.88[a]	47[a]		Disturbed silty clay
4-1, 143-144	291.93						30				Claystone
4-2, 23	292.23	1.73	1.99	1.70	1.79					3.52	Clayey siltstone
											Clayey siltstone
5-1, 90-94	405.40		1.70		1.77	1.77	30	2.62	53	3.01	Claystone
5-1, 117-120	405.67						28				Claystone
5-1, 118	405.68					1.79	29	2.64	52		Claystone
5-1, 123-128	405.73	2.31	2.13	1.92	1.91	1.89	24	2.61	45	4.13	Silty claystone
5-1, 144-149	405.94	5.22	5.05	2.68	2.64	2.47	5	2.68	13	13.58	Calcite-cemented siltstone
5-1, 144-149	405.94	5.37	5.24	2.68	2.64					14.10	Calcite-cemented siltstone (Run 2)
5-1, 144-149	405.94	5.33	5.27	2.68	2.64					14.18	Calcite-cemented siltstone (Run 3)
6-1, 138	481.88					1.69		2.52	54		Silty claystone
6-1, 138-140	481.88						32				Silty claystone
7-2, 73	519.23	1.95	1.87		1.84		29			3.44	Claystone
7-2, 88	519.38					1.92		2.57	41		Claystone
7-2, 105-109	519.55	2.76	2.37	1.92A 1.86B	2.01A[b] 1.84B		21			4.65	Silty claystone
7-2, 140-150	519.90						20				Silty claystone
8-1, 81-86	613.31	2.07	1.96	2.09	2.01					3.94	Silty claystone
8-1, 84-86	613.34					1.93	21	2.57	41		Silty claystone
8-1, 133	613.83					1.89	22	2.53	42		Claystone
8-2, 145-150	615.45						22				Claystone
9-1, 133-150	642.33						18				Silty claystone
9-2, 109-110	643.59		2.32		2.02					4.78	Sandstone
9-2, 132-133	643.82		2.04		2.01					4.18	Claystone
10-2, 0-15	710.00						15				Sandstone
10-2, 95-96	710.95		2.12		2.16					4.56	Claystone
10-2, 113-114	711.13		2.02		2.12					4.36	Sandstone
10-3, 146-147	712.96		3.56		2.37					8.65	Calcite-cemented conglomerate
10, CC	713.20	4.58	3.49	2.55	2.50					8.72	Calcite-cemented sandstone
10, CC	713.20	4.55	3.42	2.55	2.50					8.55	Calcite-cemented sandstone (Run 2)

[a]Syringe values.
[b]A = piece A; B = piece B.

INTERPRETATION OF SEISMIC PROFILES IN THE VICINITY OF SITE 325

As *Glomar Challenger* departed Site 325, it made two seismic profiler traverses within about 0.9 km of the drill hole. These profiler records and that of *Conrad*-15, which also approached within a kilometer northwest of the site, show a sediment section thicker than at Sites 322 and 323, but similar in having an upper, acoustically laminated interval overlying mostly nonlaminated sediments (Figures 4 and 8). Acoustic basement is poorly defined in the *Glomar Challenger* profile, but these records and those of *Conrad*-15 show that it is much smoother than acoustic basement normally representing basaltic crust (Figure 8).

Conrad-15 also recorded a sonobuoy profile (R-13) just northwest of the site. Careful analysis of this record indicates that the upper 0.34 sec of sediment has a velocity of 2.04 km/sec; the interval 0.34 to 0.96 sec subbottom, a velocity of 2.82 km/sec; and Layer 2 below 0.96 sec, a velocity of 5.35 km/sec. In Figure 7, the reflectors from the *Challenger* profile are placed at depths computed from these velocities. Thus the deepest distinct reflector (here called acoustic basement) is at 1024 meters, and material with velocity characteristic of basalt (5.35 km/sec) is at 1221 meters.

Acoustic basement in the *Challenger* profile near Site 325 is a reverberant horizon with its upper boundary at 0.82 sec subbottom, 0.14 sec above the probable basaltic material of Layer 2. Study of the full-scale *Conrad* record shows that coherent reflectors are present below acoustic basement (Figure 8). High-velocity sediments such as those cored shallower in the sedimentary section may overlie basaltic basement peaks, thus forming an acoustic-basement horizon which masks the basalt-sediment interface (see Herron and Tucholke, this volume; Christensen et al., 1973).

A few very faint and ill-defined reflectors appear in the nonlaminated interval above acoustic basement. The numerous silica and calcite-cemented samples recovered below 400 meters suggest that the weak reflectors in the nonlaminated interval are related to impedance contrasts caused by diagenetic changes. The acoustic impedance contrast indicated in Core 10 at 713 meters does not correspond to the sonobuoy-determined depth of any of these reflectors. However, it does match the weak reflector at 734 meters if an interval velocity of 2.66 km/sec is assumed between 0.34 sec and acoustic basement at 0.82 sec subbottom. This would require an interval velocity of 3.37 km/sec between acoustic basement and Layer 2. Both these interval velocities are reasonable in terms of the reflection rec-

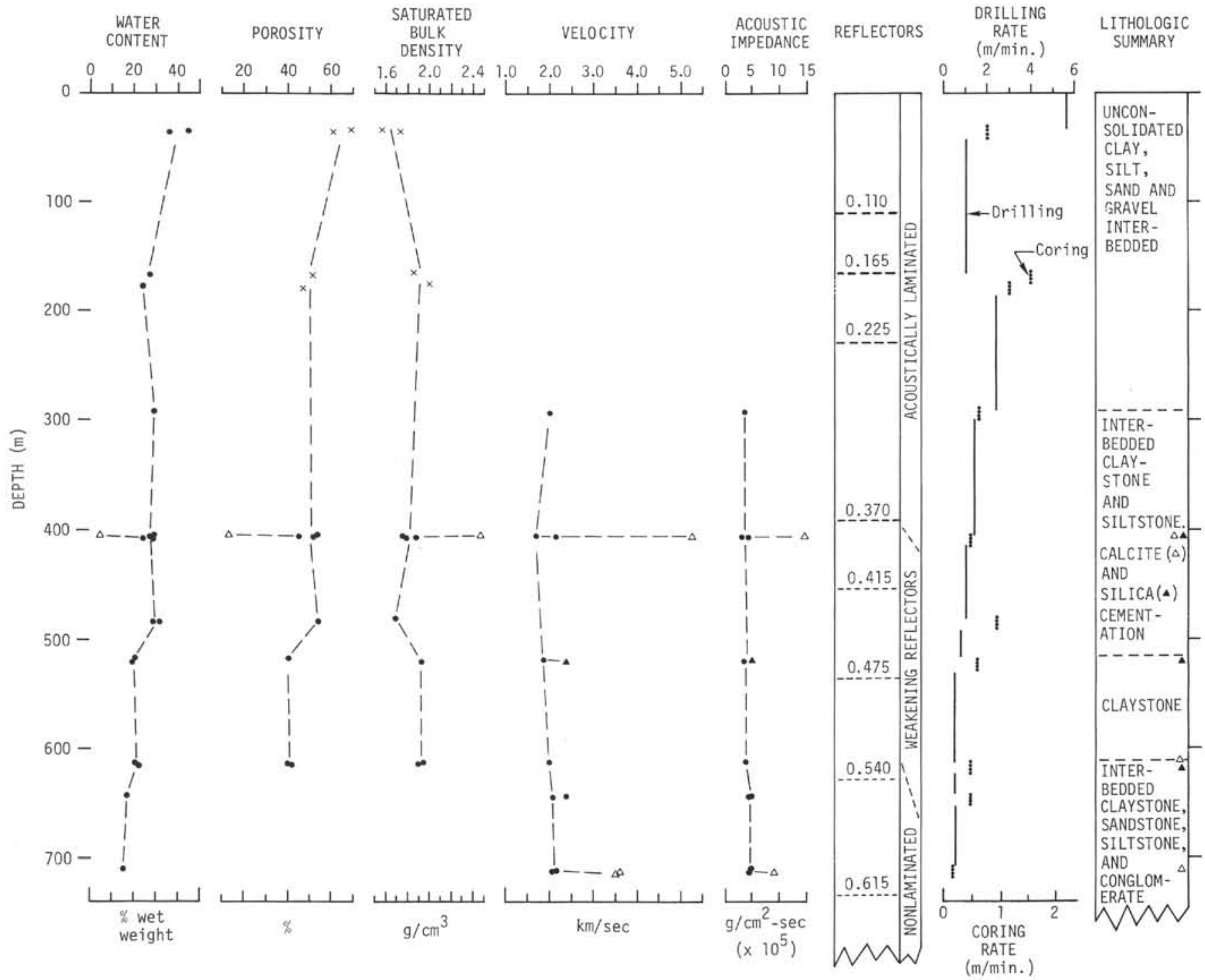

Figure 7. *Summary of physical properties, acoustic character, and lithology of sediments at Site 325. Velocities are those measured perpendicular to bedding or on unoriented samples. Relative strength of reflectors is indicated by heavy solid lines (strongest) to dotted lines (weakest), and the depth of each reflector (in seconds reflection time) is indicated. Calcite cemented samples are marked by open triangles, and cherts are solid triangles.*

ord and the sediment character, but the correlation on which they are based is too tenuous to provide much certainty in the values.

The calcite-cemented siltstone recovered at 406 meters in Core 5 provides a sharp impedance contrast which correlates reasonably well with the 0.37-sec reflector near the base of the upper, acoustically laminated interval (Figure 7). The high-velocity siltstone in this core could have come from any depth between Cores 4 and 5 because of the technique utilized throughout this interval of drilling ("washing") with an open core barrel. As an example, geochemical evidence deeper in the hole shows that Core 8 actually contains sediment from near the level of Core 7 (see Gieskes and Lawrence, this volume).

As at Sites 322 and 323, the transition from clay to claystone occurs near 300 meters, but the acoustic lamination in the profiler records extends well below this depth. However, low values of core recovery also persist to greater depths than at the first two sites, possibly suggesting that numerous beds of coarse unconsolidated material occur much deeper than the clay/claystone transition. The variations in mass physical properties between these unconsolidated and consolidated sediments may account for the deeper persistence of marked acoustic lamination.

BIOSTRATIGRAPHY

Foraminifers

Core 1 yielded a good fauna of left-coiling *Neogloboquadrina pachyderma*; Cores 2 to 6 were barren. Core 7 down to the bottom of the hole (Core 10) contains a rich fauna of arenaceous foraminifers and less abundant calcareous forms. The fauna is characterized by the primitive genera *Reophax*, *Rhabdammina*,

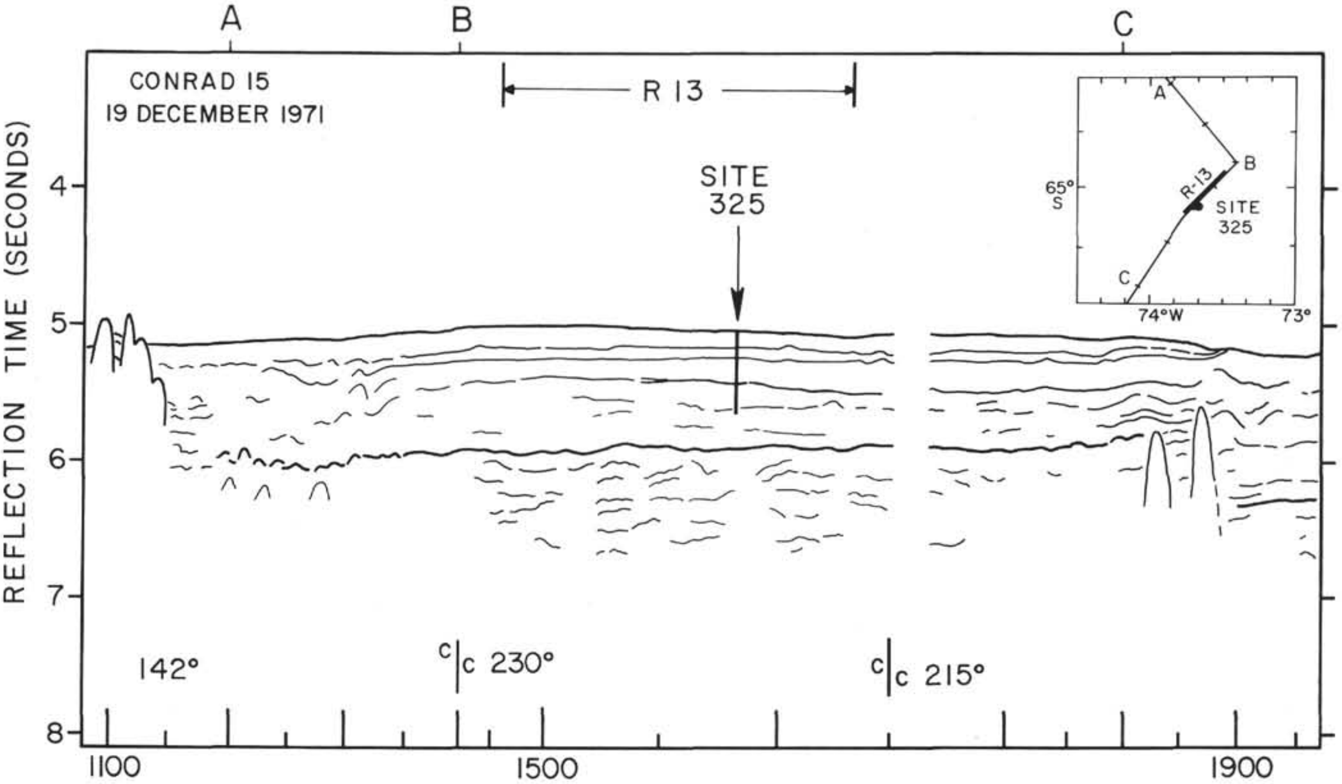

Figure 8. *Tracing of* Conrad-15 *profiler record near Site 325. Sonobuoy (R-13) location is shown.*

Rhizammina, and *Saccammina*, and the stratigraphically important arenaceous species are *Cyclammina incisa*, *C. japonica*, *C.* cf. *rotundata*, and *Haplophragmoides carinatus*. Of the calcareous species *Laticarinina pauperata* is the most significant. In Sample 325-10-1, 94-96 cm *Globorotalia zealandica incognita* was present which, according to Berggren and Amdurer (1973), ranges from late N6 to early N7 zones (late early Miocene).

Calcareous Nannoplankton

No calcareous nannoplankton were found in Cores 1 through 6. Nannofossils are common to abundant in Core 7, but they are generally very poorly preserved and at some levels show considerable recrystallization. It is difficult to distinguish species except at some levels which yield better preserved specimens. Both Cores 7 and 8 contain similar assemblages composed dominantly of *Ericsonia ovalis*, *Dictyoccites* sp., *D.* aff. *scrippsae* and to a lesser degree of *Reticulofenestra* aff. *pseudoumbilica*. This overall composition of the flora indicates that these cores are Oligocene-Miocene in age.

Cores 9 and 10 are devoid of nannofossils.

Bolboforma

Extremely large numbers of *Bolboforma* were found in Sample 325-8-2, 133-135 cm. The species are *Bolboforma clodiusi*, *B. laevis*, *B.* cf. *rotunda*, and *B. spinosa*. By comparison to previously reported occurrences of *Bolboforma* from northern Germany, the age of this assemblage is early Miocene (see also Rögl, this volume).

Radiolarians

Radiolarians were found in all cored intervals at Site 325. Preservation is poor to moderate and species abundances and diversity are generally low. Cores 7, 8, 9, and 10 contain abundant radiolarians, but diagenetic effects within the claystones have resulted in partial or complete test recrystallization. Identification and age determinations within these intervals were therefore difficult and may be unreliable.

Core 1, Section 1 (18-20 cm) through Sample 3, CC contains a typical Pliocene radiolarian assemblage and can be assigned to the *Helotholus vema* Zone of Chen (1975) (Table 3). Species include *Antarctissa denticulata*, *A. strelkovi*, *Spongotrochus glacialis*, *Spongodiscus osculosus*, *Triceraspyris antarctica*, *Saccospyris antarctica*, *Prunopyle tetrapila*, *P.* (?) *titan*, *Lithelius nautilioides*, *Cornutella profunda*, *Desmospyris spongiosa*, *Eucyrtidium calvertense*, and *Helotholus vema*. Although the index species *H. vema* occurs only sporadically throughout this interval, *D. spongiosa*, which has approximately the same stratigraphic range as *H. vema*, does occur consistently through the entire interval, thus restricting it to the Pliocene.

Samples 325-4, CC; 325-5-1, 102-104 cm; 325-5, CC; and 325-6, CC are assigned to the *Theocalyptra bicornis spongothorax* Zone of Chen (1975). The top of this zone is placed between 325-3, CC and 325-4, CC at the first occurrence of *Helotholus vema*. Although *Theocalyptra bicornis spongothorax* only occurs in Sample 5, CC, the co-occurrence of the Pliocene form of *Stylatractus universus*, *Prunopyle hayesi*, *Stichocorys* (?) *peregrina*, *Ant-*

TABLE 3
Occurrence of Radiolarians at Site 325

Sample (Interval in cm)	Abundance	Preservation	Age	Zone	*Antarctissa denticulata*	*A. strelkovi*	*A. conradae*	*A. antedenticulata*	*Spongotrochus glacialis*	*Spongodiscus osculosus*	*Prunopyle antarctica*	*Triceraspyris antarctica*	*Siphocampe aquilonaris*	*Saccospyris antarctica*	*Saccospyris conithorax*	*Stylatractus neptunus*	*Prunopyle tetrapila*	*Lithelius nautiloides*	*Stylodictya validispina*	*Lithomitra arachnea*	*Cornutella profunda*	*Stylatractus universus*	*Saturnalis circularis*	*Spongurus pylomaticus*	*Theocalyptra bicornis*	*Desmospyris spongiosa*	*Helotholus vema*	*Eucyrtidium calvertense*	*E.* sp. aff. *E. inflatum*	*E. cienkowskii* group	*Dendrospyris haysi*	*Stichocorys peregrina* (?)	*Theocalyptra bicornis spongothorax*	*Triceraspyris coronatus*	*Cannartus* sp. aff. *C. prismaticus*	*C.* sp. aff. *C. mammiferus*	*Prunopyle titan*	*Prunopyle hayesi*
325-1-1, 25-27																	Barren																					
325-1-1, 41-43																	Barren																					
325-1-1, 89-91																	Barren																					
325-1-1, 123-125																	Barren																					
325-1-2, 18-20	R	M	Pliocene	*Helotholus vema*	R	–	–	–	R	–	–	–	–	–	–	–	–	–	–	–	–	–	–	–	–	–	–	–	–	–	–	–	–	–	–	–	–	–
325-1-2, 49-51	F	M			R	R	–	R				R	–	–	–	F	–	F	–	–	–	–	–	–	–	R	–	–	–	–	–	–	–	R	–	–	R	–
325-1-2, 89-91	F	M			F	R	–	–	R	–	–	R	–	R	–	F	–	F	R	–	–	–	–	–	–	–	–	–	–	–	–	–	–	R	–	–	–	–
325-1-2, 115-117	F	M			F	–	–	–	R	–	R	R	R	R	R	F	–	R	R	–	–	–	–	–	–	R	–	–	–	–	–	–	–	R	–	–	–	–
325-1-2, 147-149	R	P			R	–	–	–	–	–	–	–	–	–	–	–	–	–	–	–	–	–	–	–	–	–	–	–	–	–	–	–	–	–	–	–	–	–
325-1-3, 13-15	R	P			–	–	–	–	–	–	–	–	–	–	–	–	–	R	–	–	–	–	R	–	–	–	–	–	–	–	–	–	–	–	–	–	–	–
325-1-3, 44-46	F	M			R	–	–	–	–	–	–	–	R	–	–	R	–	–	R	–	–	–	–	–	–	R	–	–	–	–	–	–	–	–	–	–	–	–
325-1-3, 58-60																	Barren																					
325-1-3, 104-106	R	P			R	R	–	–	–	–	–	R	R	–	–	R	–	–	–	–	–	–	–	–	–	–	–	–	–	–	–	–	–	–	–	–	–	–
325-1-3, 125-127	R	P			–	–	–	–	–	R	–	–	R	–	–	–	–	–	–	–	–	–	–	–	–	R	–	–	–	–	–	–	–	–	–	–	–	–
325-1-4, 33-35	R	P			R	–	–	–	–	–	–	–	–	R	–	–	–	–	–	–	–	–	–	–	–	–	–	–	–	–	–	–	–	–	–	–	–	–
325-1-4, 96-98	R	P			–	–	–	–	–	–	–	–	–	–	–	–	R	–	–	–	–	–	–	–	–	–	–	–	–	–	–	–	–	–	–	–	–	–
325-1-4, 136-138	R	M			–	R	–	R	R	–	–	–	R	–	–	–	–	R	–	–	–	–	–	–	–	R	–	–	–	–	–	–	–	–	–	–	–	–
325-1-4, 144-146	C	M			C	F	–	R	F	C	–	–	R	R	–	–	–	R	R	–	–	–	–	–	–	C	R	R	–	–	–	–	–	–	–	–	R	–
325-1, CC	F	M			F	R	R	R	R	R	–	–	–	–	–	–	–	–	–	–	–	–	–	–	–	C	–	R	–	–	–	–	–	–	–	–	–	–
325-2-1, 142-144	F	M			R	R	–	–	–	–	R	–	–	–	–	–	–	–	–	–	–	–	–	R	–	F	R	–	–	–	–	–	–	–	–	–	–	–
325-2-2, 76-78	R	P			R	R	–	–	–	–	–	–	–	–	–	–	–	–	–	–	–	–	–	–	–	R	–	–	–	–	–	–	–	–	–	–	–	–
325-2-2, 112-114	F	M			F	R	–	–	F	–	–	–	–	R	–	–	–	R	–	–	–	–	–	–	–	R	R	R	–	–	–	–	–	–	–	–	R	–
325-2-2, 146-148	R	M			–	R	–	–	–	–	–	–	–	R	–	–	–	–	–	–	–	–	–	–	–	–	–	–	–	–	–	–	–	–	–	–	–	–
325-2, CC	R	M			R	R	–	–	R	–	–	–	–	–	–	–	–	–	–	–	–	–	–	–	–	R	R	R	–	–	–	–	–	–	–	–	–	–
325-3-1, 123-125	F	M			F	R	–	R	R	R	–	–	–	R	–	–	–	–	–	R	R	–	–	–	–	C	–	–	–	–	–	–	–	–	–	–	–	–
325-3-2, 43-45	R	P			R	–	–	–	–	–	–	–	–	–	–	–	–	–	–	–	–	–	–	–	–	R	–	R	–	–	–	–	–	–	–	–	–	–
325-3-2, 105-107	F	M			F	–	–	–	R	–	R	–	–	–	–	–	–	–	–	–	–	–	–	–	–	F	R	R	–	–	–	–	–	–	–	–	–	–
325-3-3, 43-45	F	M			F	F	–	–	R	–	–	–	–	R	R	–	–	–	–	–	–	–	–	–		R	R	R	–	–	–	–	–	–	–	–	–	–
325-3-3, 103-105	F	M			C	F	–	–	–	R	R	–	–	R	–	–	–	–	–	R	R	–	–	–	–	F	R	R	–	–	–	–	–	–	–	–	–	–
325-3-4, 45-47	F	M			F	R	–	–	R	R	–	–	–	F	–	–	–	–	–	–	–	–	–	–	–	F	R	R	–	–	–	–	–	–	–	–	–	–
325-3-4, 106-108	F	M			F	R	–	–	R	–	–	–	–	R	–	–	–	–	–	R	–	–	–	–	–	C	R	R	–	–	–	–	–	–	–	–	–	–
325-3, CC	F	M			F	R	–	–	R	F	–	–	–	R	R	R	–	–	–	R	–	–	–	–	–	C	R	F	–	–	–	–	–	–	–	–	–	–
325-4, CC	F	M		*T. D. Spongothorax*	F	–	R	R	–	R	–	–		–	–	–	–	–	–	–	R	–	–	–	–	R	–	R	R	–	–	R	–	–	–	–	–	–
325-5-1, 102-104	F	M			–	–	–	–	–	R	–	–	–	–	–	–	–	–	–	–	–	F	–	–	–	R	–	R	–	–	–	–	–	–	–	–	–	F
325-5, CC	R	M			–	–	–	–	–	–	–	–	–	–	–	–	–	–	–	–	–	F	–	–	–	–	–	–	–	–	R	–	R	–	–	–	–	F
325-6, CC	R	M			–	–	–	–	–	R	–	–	–	–	–	–	–	–	–	–	–	–	–	–	–	–	–	R	–	–	R	–	–	–	–	–	–	R
325-7-1, 105-140	C	P	L. Mio.					Silica Recrystallized																						–					–	–		–
325-7-2, 51-53	C	P						Silica Recrystallized																						–					–	–		–
325-7, CC	A	P						Silica Recrystallized																						–					–	–		–
325-8-1, 51-53	A	P	E.-M. Miocene					Silica Recrystallized																						F					–	–		–
325-8-1, 90-92	A	P						Silica Recrystallized																						F					–	–		–
325-8-2, 118-120	C	P						Silica Recrystallized																						–					–	–		–
325-8-3, 10-12	C	P						Silica Recrystallized																						F					–	–		C
325-8, CC	C	P						Silica Recrystallized																						–					–	–		–
325-9-1, 128-131	R	P						Silica Recrystallized																						F					–	R		–
325-9-2, 3-6	C	P						Silica Recrystallized																						–					–	–		–
325-9-2, 80-83	C	P						Silica Recrystallized																						F					–	F		–
325-9-2, 110-113	C	P						Silica Recrystallized																						F					–	F		–
325-9-3, 49-53	C	P						Silica Recrystallized																						–					–	–		–
325-9-3, 85-87	C	P						Silica Recrystallized																						–					–	R		–
325-9-3, 137-139	R	P	Olig. to E. Mio.					Silica Recrystallized																						–					–	–		–
325-9, CC	A	P						Silica Recrystallized																						–					–	–		–
325-10-1, 89-91	C	P						Silica Recrystallized																						–					R	F		–
325-10-2, 90-92	C	P						Silica Recrystallized																						F					–	–		–
325-10-3, 56-58	C	P						Silica Recrystallized																						–					–	–		–
325-10, CC	C	P						Silica Recrystallized																						–					–	R		–

arctissa conradae, and *A. antedenticulata* (see Table 3), throughout the other samples examined within this interval, restricts them to the *T.b. spongothroax* Zone of Chen.

Radiolarian age determinations from material recovered from Cores 7 through 10 are difficult due to recrystallization of the faunal assemblages present. Two species could positively be identified within this interval, *Eucyrtidium cienkowskii* group and *Prunopyle hayesi* (Table 3). Cores 9 and 10 contain recrystallized specimens of what appears to be *Cannartus mammiferus*, based on their rough morphological appearance. Most details are obscured, but what may be remanent protuberances can be seen on the sides of the cortical shells of many specimens. (See pl. 5, fig. 8 of Weaver, this volume.) Sample 10-1, 90-92 cm contains several specimens closely resembling *Cannartus prismaticus* (pl. 5, fig. 9 in Weaver, this volume.)

If these identifications are correct, Cores 9 and 10 could possibly range in age from upper Oligocene through the middle Miocene, based upon the defined ranges of *Cannartus mammiferus* and *C. prismaticus* in lower latitudes.

Silicoflagellates

Silicoflagellates were found only in Cores 2 and 3. The assemblage consists of commonly occurring *Distephanus speculum* (short-spined variety), and a few other more rarely occurring forms. From the overall composition of the assemblage, this material can be assigned to the mid-Pliocene *Distephanus boliviensis* Zone.

Diatoms

Diatoms are present in all cores recovered at Site 325. Those in Cores 1-6 comprise a low diversity Antarctic assemblage with moderately to poorly preserved frustules. Those in Cores 7-10, however, are pyritized and do not yield an age determination. Core 1, Sections 2 and 3 only contained a badly preserved assemblage and age-diagnostic fossils were rare. The first occurrence of *Nitzschia kerguelensis* places this sample into the upper part of the Pliocene with an age of less than 2.43 m.y.B.P. Sample 1-4, 140 cm through Sample 3-4, 104 cm contained *Nitzschia interfrigidaria* and *Coscinodiscus insignis*, which are characteristic fossils of the *Nitzschia interfrigidaria* Partial Range Zone of McCollum (1975). This has been correlated to the paleomagnetic stratigraphy with its top near the Kaena event (2.85 m.y.B.P.) and the base above the "A" event within the reversed Gilbert magnetic epoch (3.65 m.y.B.P.). Sample 3, CC is tentatively placed within the *Nitzschia praeinterfrigidaria* Partial Range Zone of McCollum (1975), the base of which has been correlated to the "C" event of the Gilbert epoch (approximately 4.5 m.y.B.P.) and the top near the "A" event of the Gilbert epoch (3.65 m.y.B.P.). Samples below this level are placed within the Miocene, however, a correlation to the established Miocene zonation on the basis of the sparsely recovered and poorly preserved material is impossible.

RATES OF SEDIMENT ACCUMULATION

Sediment accumulation rates for Site 325 are summarized in Figure 9. Precise age limits cannot be established on most cores, especially the Miocene material recovered in Cores 4-10. Four significant changes in the rate of sediment accumulation from the mid-Tertiary to Recent are recorded at Site 325 (Figure 9). Core 1, which was recovered at 30 meters, lies within the Upsion radiolarian Zone of Hays (T = ~2.4 to 4.0 m.y.B.P.) thus, an average sedimentation rate of about 1 cm/1000 yr is indicated for the uppermost 30 meters of the sequence. A much higher accumulation rate is recorded between Cores 1 and 6 (late Miocene to early Pliocene). 450 meters of sediment accumulated during approximately 1.5 m.y. yielding a rate of accumulation of 9 cm/1000 yr. As at Sites 322 and 323, where high accumulation rates are recorded throughout the early Pliocene, this anomalously high rate, for essentially the same time interval at Site 325, may be related to a period of increased continental erosion throughout West Antarctica.

The available age data indicate that the middle Miocene is either missing or highly compressed at this site. Maximum rates of accumulation are about 0.3 cm/1000 yr.

Based on an early Miocene (19 to 17 m.y.) age of Cores 7 to 10 (about 15-17 m.y.), the average accumulation rate in this interval is about 10 cm/1000 yr., comparable to that in late Miocene/early Pliocene sediments higher in the hole.

SUMMARY AND CONCLUSIONS

Summary

Site 325 is located at 65°02.79'S, 73°40.40'W on the central continental rise northwest of the Antarctic Peninsula about 80 miles from the base of the continental slope. The single hole drilled at this site reached a total depth of 718 meters before adverse sea conditions and resulting ship motion forced its abandonment. The entire sequence penetrated consists of Cenozoic sedimentary deposits, and the oldest fossiliferous beds are of Oligocene to early Miocene age. A total of 95 meters was cored and 34.4 meters (36.2%) of core were recovered. Time on station at this site was 103 hr.

The sedimentary sequence consists mostly of terrigenous turbidite and ice-rafted detritus except for a few thin beds with mainly biogenic components. Although recovered cores represent less than 5% of the entire sequence, it can be divided into two lithologic units. The upper limit is about 570 meters thick, and its basal contact falls between Cores 7 and 8. Clay and claystone are dominant over siltstone and sandstone in this unit. Quartz silt occurs both as thin layers or laminae and disseminated in the clay. Ice-rafted pebbles and coarse sand grains are abundant in the upper part of the unit, and isolated pebbles within claystone occur as low as Core 7 (Figure 10).

The lower unit is at least 150 meters thick, and it consists of dominant coarser clastic rocks with minor amounts of claystone. Sandstones are abundant and

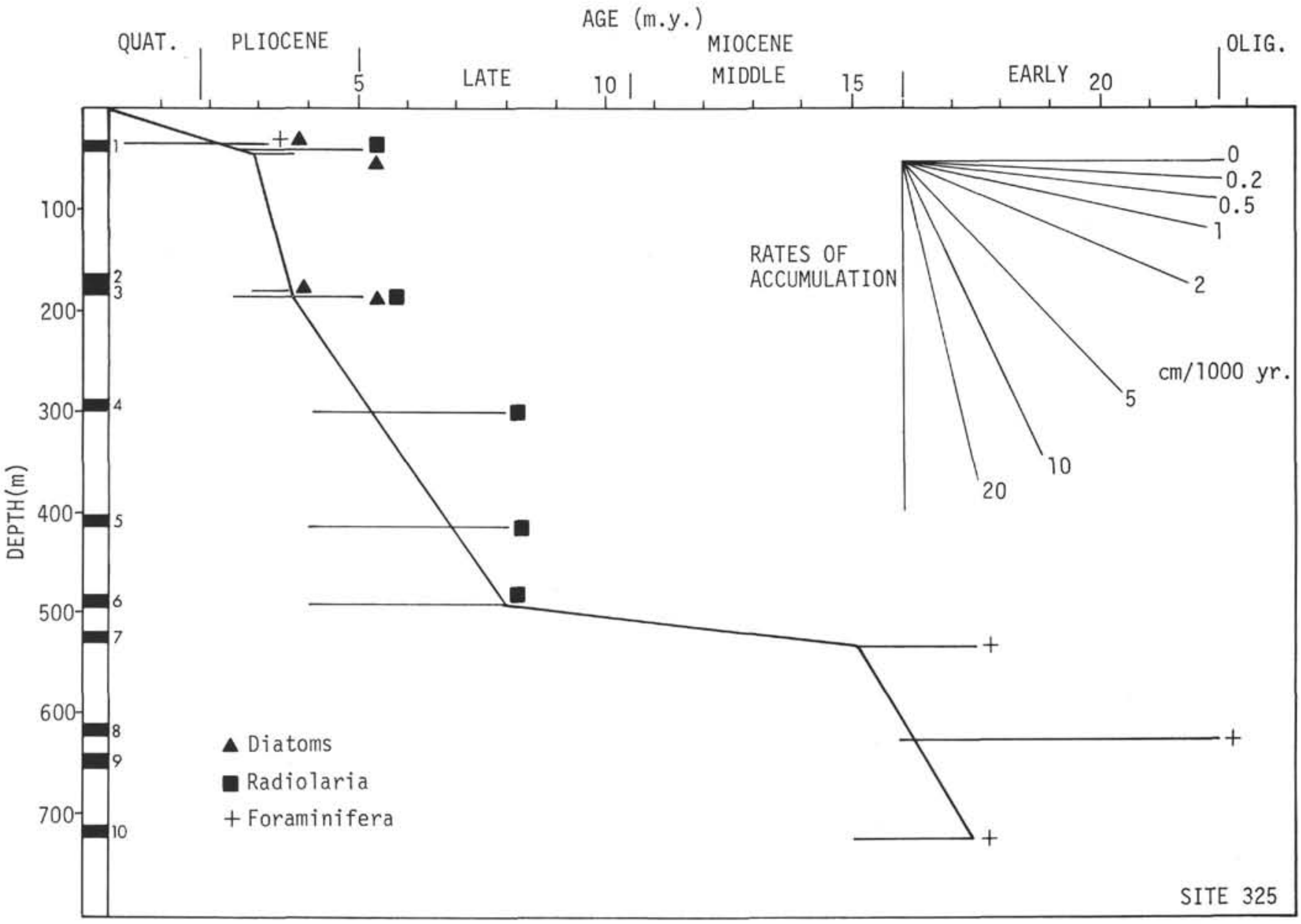

Figure 9. *Rates of sediment accumulation, Site 325.*

consist mainly of quartz and rock fragments. Several conglomerates with clay clasts occur in Core 10.

All 10 cores from Site 325 contain fossils, and all five major microfossil groups are present in the sequence. Diatoms are the most abundant and occur in each core. Those in Cores 1-6 comprise a low diversity Antarctic assemblage ranging in age from late Pliocene to late Miocene. Unfortunately, the diatoms in Cores 7-10 are pyritized and do not yeild an age. Radiolarians occur in all cores. Those in Cores 1-6 are Pliocene to late Miocene, but those from Core 7 downward are too recrystallized to provide a definite age. Cores 2-6 are barren of foraminifers, but Core 1 contains a good Pliocene-Pleistocene fauna of *Neogloboquadrina pachyderma*. Cores 7-10 contain calcareous and arenaceous foraminfers of early Miocene age. Core 10 is dated by forams as early Miocene. Oligocene-Miocene nannoplankton are abundant in a few thin calcareous beds in Cores 7 and 8. A few silicoflagellates are present in Cores 2 and 3 indicating a mid-Pliocene age. Figure 11 presents a lithologic and biostratigraphic summary of Site 325.

Samples were taken from nine cores for geochemical studies. Measurements were obtained of formation factor, water content, porosity, and certain chemical properties. Downhole increases were noted in formation factor, *p*H, and dissolved calcium, along with decreases in porosity, water content, and dissolved silica and magnesium. Alkalinity reaches a maximum at 200 meters and decreases at greater depths. Dissolved ammonia follows the same pattern, reaching a maximum at about 400 meters. In general the geochemistry data suggest that significant postdepositional alteration reactions occurred in the sediment of 325.

Conclusions

1. Turbidity current deposition along with ice rafting are the two dominant processes of sedimentation at this site.

2. The percentage of quartz embedded within the clay and claystone varies inversely with the frequency of silt laminae. The quantity of quartz silt supplied to this region has apparently been constant, and the variation in mode of occurrence is probably directly related to the presence or absence of contour currents.

3. An accumulation rate of 12-15 cm/1000 yr calculated for early to middle Pliocene suggests vigorous continental erosion during this time. Similar high rates were also found at Sites 322 and 323 for the same period.

4. The oldest ice-rafted debris occurs in lower Miocene claystone, which agrees well with the age of

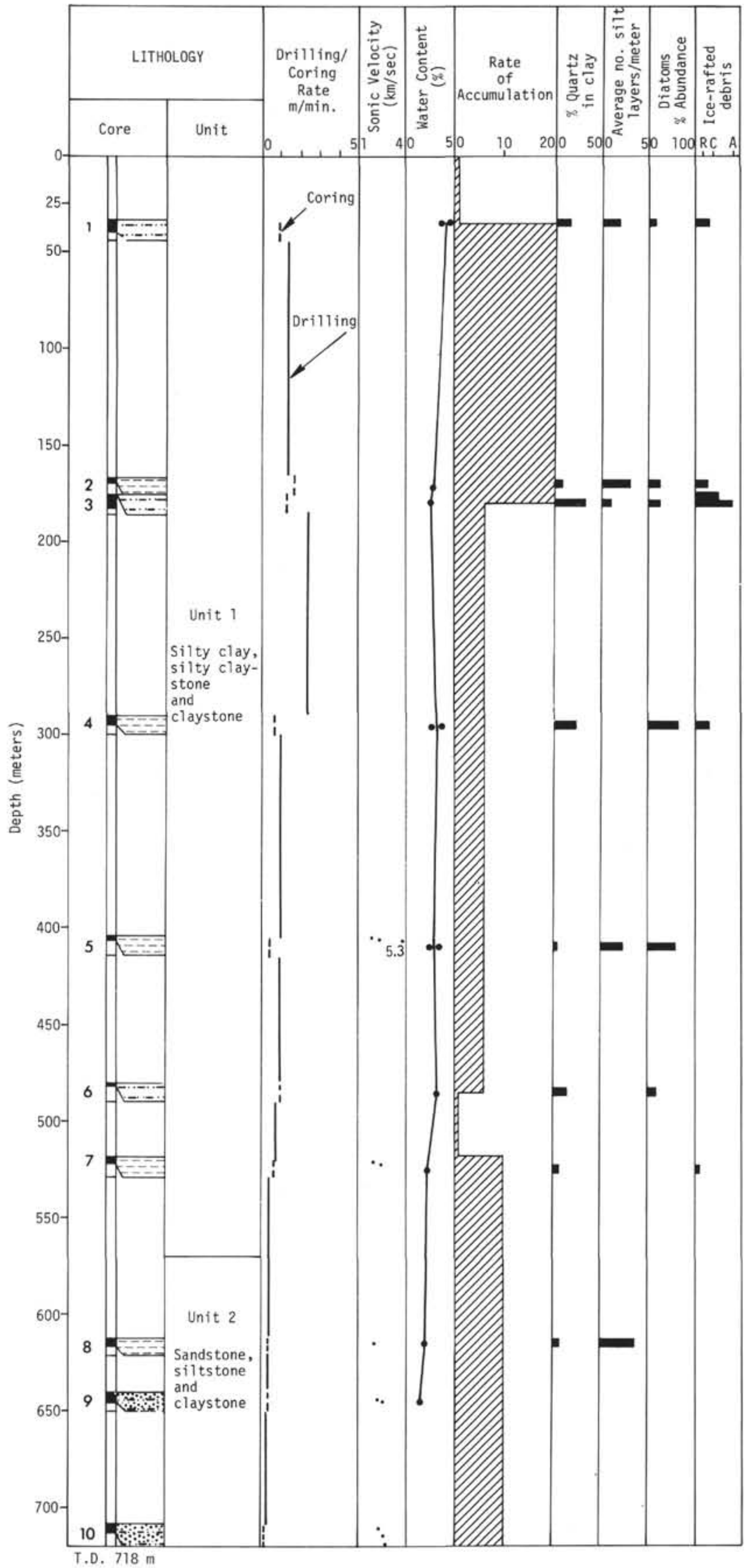

Figure 10. *Summary of lithology, lithologic components, accumulation rates, and physical properties, Site 325.*

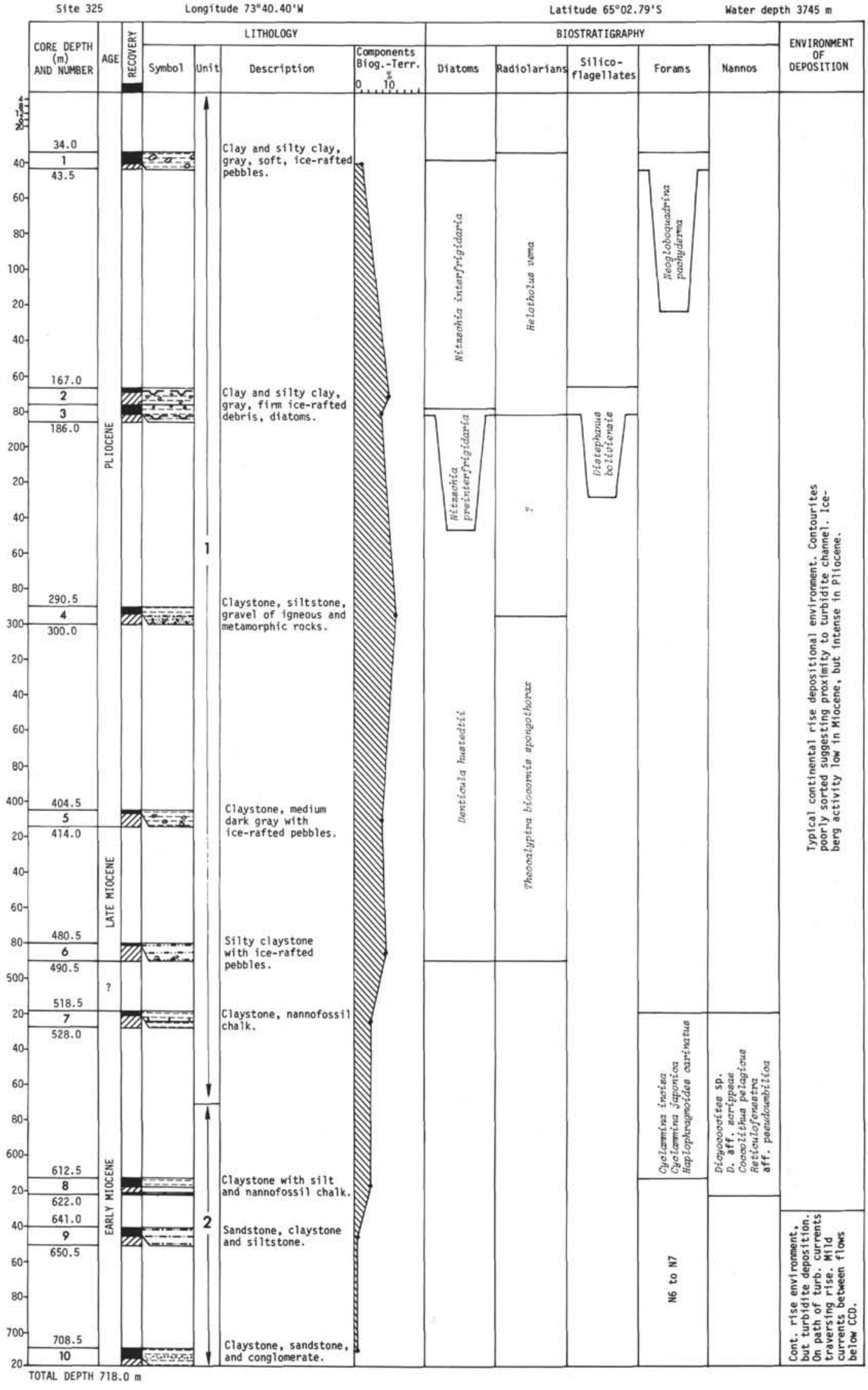

Figure 11. *Lithologic and biostratigraphic summary, Site 325.*

the first occurrence of ice-rafted sediment in a similar deep-sea environment encountered during Leg 28 just off East Antarctica. However, ice-rafted debris on both Legs 28 and 35 at sites north of about 63°S occur only in post-Miocene deposits.

5. Geochemistry data show that there is a source for calcium and sink for magnesium within the upper sediments and, in general, the data suggest that postdepositional alteration reactions of volcanic debris are significant in these sediments.

6. The high velocity (5.3 km/sec) calcite-cemented siltstone from 406 meters appears to correlate well with a 0.37-sec reflector near the base of the upper acoustically laminated sequence.

REFERENCES

Adie, R.J., 1970. Antarctic Peninsula (Plate I, II). Geologic maps of Antarctica, Folio 12, Antarctic Map Folio Series: New York (Am. Geogr. Soc.).

Berggren, W.A., and Amdurer, M., 1973. Late Paleogene (Oligocene) and Neogene planktonic foraminiferal biostratigraphy of the Atlantic Ocean (lat. 30°N, to Lat. 30°S): Riv. Ital. Paleont., v. 79, p. 337-392.

Bouma, A.H., 1962. Sedimentology of some flysch deposites: Amsterdam (Elsevier).

Christensen, N.I., Fountain, D.M., and Steward, R.J., 1973. Oceanic crustal basement: a comparison of seismic properties of DSDP basalts and consolidated sediments: Marine Geol., v. 15, p. 215-226.

Chen, P., 1975. Antarctic Radiolaria, Leg 28, Deep-Sea Drilling Project. *In* Frakes, L.H., Hayes, D.E., et al., Initial Reports of the Deep Sea Drilling Project, Volume 28: Washington (U.S. Government Printing Office), p. 437-513.

Craddock, C., 1972. Geologic map of Antarctica, scale 1:5,000,000: New York (Am. Geogr. Soc.).

Craddock, C., Bastien, T.W., and Rutford, R.H., 1964. Geology of the Jones Mountains. *In* Adie, R.J. (Ed.), Antarctic geology: Amsterdam (North Holland Pub. Co.), p. 171-187.

Dalziel, I.W.D. and Elliot, D.H., 1973. Scotia Arc and Antarctic margin. *In* Nairn, A.E.M. and Stehli, F.G. (Eds.), The ocean basins and margins, vol. 1: New York (Plenum Pub. Corp.), p. 171-246.

Gordon, A.L., 1967. Structure of Antarctic waters between 20°W and 170°W, Folio 6, Antarctic Map Folio Series: New York (Am. Geogr. Soc.).

———, 1972. On the interaction of the Antarctic circumpolar current and the Macquarie Ridge. *In* Antarctic Oceanology II, Antarctic Res. Ser.: Am. Geophys. Union, p. 71-78.

Hollister, C.D. and Heezen, B.C., 1967. The floor of the Bellingshausen Sea. *In* Hercey, J.B. (ed.), Deep sea photography: Baltimore (John Hopkins Univ. Press).

———, 1972. Geologic effects of ocean bottom currents. *In* Gordon, A.L. (ed.), Studies in physical oceanography, Volume 2: New York (Gordon & Breach), p. 37-66.

Kennett, J.P., Burns, R.E., Andrews, J.E., Churkin, M., Jr., Davies, T.A., Dumitrica, P., Edwards, A.R., Galehouse, P., Packham, G.H., van der Lingen, G.J., 1972. Australian-Antarctic continental drift, paleocirculation changes and Oligocene deep sea erosion: Nature, v. 239, p. 51-55.

LeMasurier, W.E., 1972. Volcanic record of Cenozoic glacial history of Maries Byrd Land. *In* Adie, R.J. (Ed.), Antarctic geology and geophysics: Oslo (Universitetsforlaget), p. 251-259.

McCollum, D.W., 1975. Leg 28 diatoms. *In* Frakes, L.A., Hayes, D.E., et al., Initial Reports of the Deep Sea Drilling Project, Volume 28: Washington (U.S. Government Printing Office), p. 515-571.

Margolis, S.V. and Kennett, J.P., 1970. Antarctic deep sea cores: Science, v. 170, p. 1805-1087.

Reid, J.L. and Nowlin, W., 1971. Transport of water through the Drake Passage: Deep-Sea Res., v. 18, p. 51-64.

Rutford, R.H., Craddock, C., White, C.M., and Armstrong, R.L., 1972. Tertiary glaciation in the Jones Mountains. *In* Adie, R.J. (Ed.), Antarctic geology and geophysics: Oslo (Universitetsforlaget), p. 239-243.

Weissel, J.K. and Hayes, D.E., 1972. Magnetic anomalies in the southeast Indian Ocean. *In* Antarctic Oceanology II, Antarctic Res. Ser.: Am. Geophys. Union, p. 165-196.

Hole 325, Core 1 Cored Interval: 34.0-43.5 m

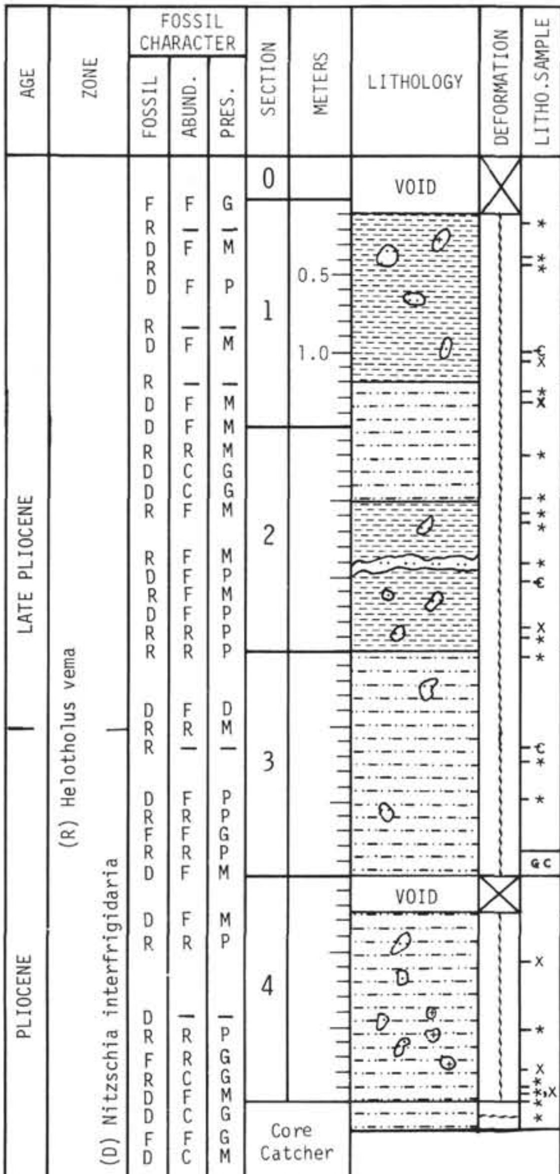

LITHOLOGIC DESCRIPTION

CLAY AND QUARTZ SILTY CLAY

CLAY: gray (2.5Y 5/0), soft, sticky, with pockets and lenses of quartz silt. One ice-rafted igneous pebble, many other small fragments. Composition: 81% clay mins., 15% qtz., 2% heavy mins., 1% diatoms, traces rads, fldspr, opaque mins., authigenic carbonate, hematite, recrystallized silica. Carbon/carbonate: 1-97 (0.2-0.1-0.0).

QUARTZ-SILTY CLAY: gray (5Y 4/1) to olive gray (5Y 5/1), soft, sticky, poorly sorted mainly angular quartz. Composition: 50-78% clay mins., 20-34% qtz., 0-5% rock frags., traces diatoms, rads, forams, nannos, pyrite, auth. carb., fldspr., mica, hematite, opaque mins.

CLAY: gray (2.5Y 5/0), some mixing of olive and brown. Soft, sticky with pockets and lenses of disturbed, poorly sorted quartz silt. Compostion: 55-74% qtz., 4-10% rock frags., 0-10% clay mins., 5-7% heavy mins., 2-5% fldspr., 1-5% auth. carbonate. Carbon/carbonate: 2-103 (0.3-0.1-1.0).

SILTY CLAY: olive gray (5Y 5/1) to medium dark gray (N4), mottled, pods of poorly to well sorted silt. Composition: 92% clay mins., 7% qtz., traces heavy and opaque mins., fldspr., hematite, diatoms. Carbon/carbonate: 3-65 (0.2-0.1-0.0).

SILTY CLAY: dark gray (N4), soft, sticky, highly disturbed, with pods of silt and four pebbles of ice-rafted felsite. Composition: 52-83% clay mins., 15-35% qtz., 1-5% heavy mins., tr-5% fldspr., 0-2% rock frags., tr-10% diatoms. Dramatic color changes between 137-150 cm including beds of dark greenish gray (5GY 4/1), dusky blue green (5BG 4/2), but no charistic difference in lithology.

CLAYEY QUARTZ-SILT: gray (N4), poorly sorted. Composition: 65% qtz., 30% clay mins., 3% heavy mins., 2% diatoms.

BULK X-RAY

	1: 103-106	1: 130-132	2: 131-134
Amorph.	54.5%	52.7%	49.5%
Crystal.	45.5%	47.3%	50.5%
Percent of Crystalline Component			
Quartz	21.4%	20.0%	22.0%
K-Fldspr.	14.1%	12.1%	10.2%
Plag.	28.9%	28.5%	30.5%
Mica	12.7%	16.9%	14.2%
Chlorite	6.6%	6.4%	5.8%
Mont.	13.2%	12.1%	14.6%
Clinop.	0.7%	0.7%	0.4%
Amphi.	2.3%	3.3%	2.4%

	4: 131-133	4: 143-144
Amorph.	39.8%	57.1%
Crystal.	60.2%	42.9%
Percent of Crystalline Component		
Quartz	29.3%	21.0%
K-Fldspr.	15.7%	6.0%
Plag.	36.7%	37.9%
Mica	5.5%	7.0%
Chlorite	4.2%	6.0%
Mont.	5.1%	17.0%
Clinop.	0.5%	0.4%
Amphi.	3.0%	4.7%

Explanatory notes in Chapter 2

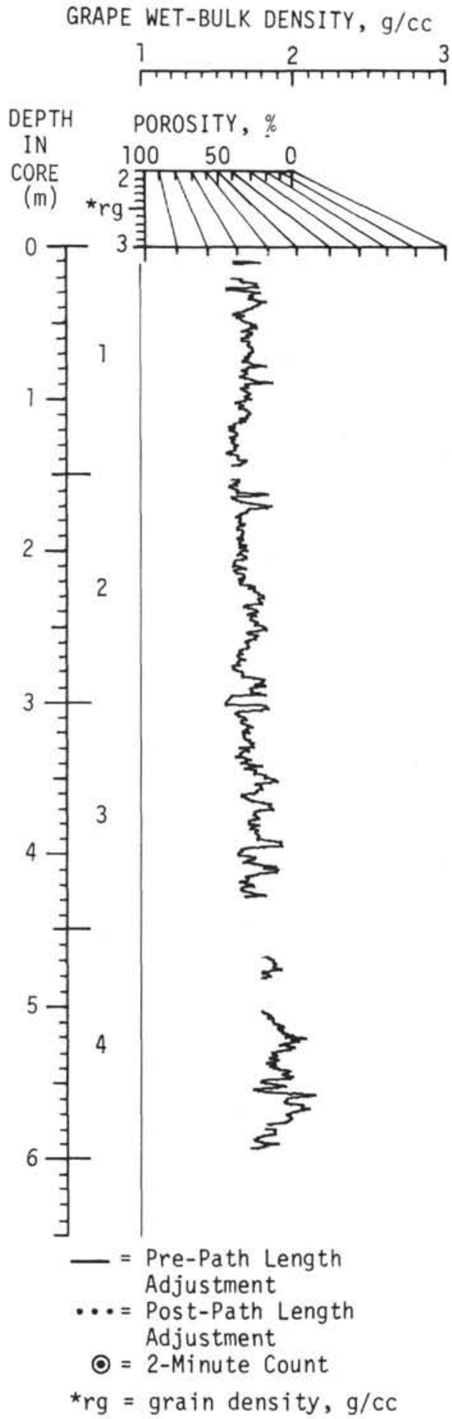
GRAPE WET-BULK DENSITY, g/cc
1
2
3
DEPTH IN CORE (m)
POROSITY, %
100
50
0
*rg
0
1
2
3
4
5
6
— = Pre-Path Length Adjustment
••• = Post-Path Length Adjustment
⊙ = 2-Minute Count
*rg = grain density, g/cc

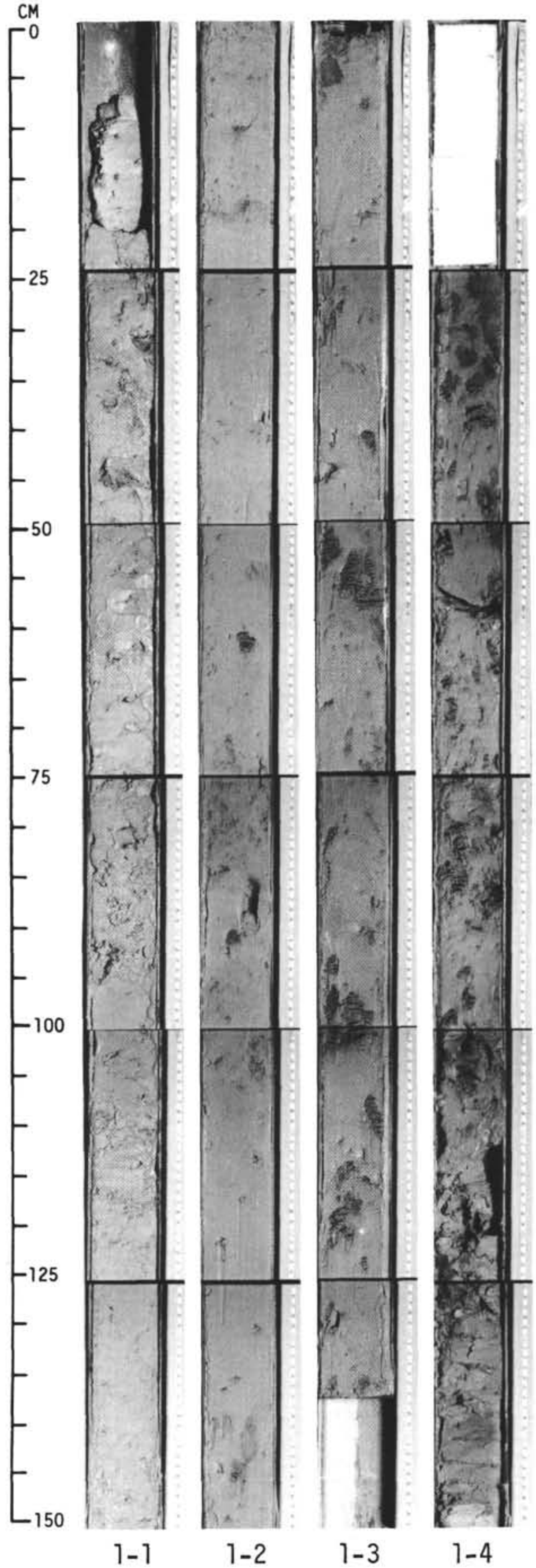
CM
0
25
50
75
100
125
150
1-1
1-2
1-3
1-4

Hole 325, Core 2 Cored Interval:167.0-176.5 m

AGE	ZONE	FOSSIL CHARACTER: FOSSIL	ABUND.	PRES.	SECTION	METERS	LITHOLOGY	DEFORMATION	LITHO. SAMPLE
PLIOCENE	(R) Helotholus vema (D) Nitzschia interfrigidaria	D R D	D F C	D M M	0		VOID		
		D R	C R	M P	1	0.5 1.0			GC
		D R	C F	M M	2				* x * *
		D R R D	C R R C	M M M M	Core Catcher				*

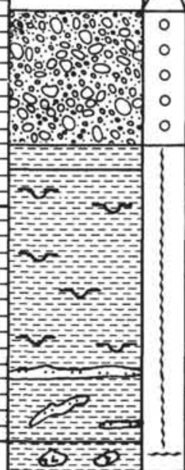

LITHOLOGIC DESCRIPTION

GRAVEL AND DIATOM-BEARING CLAY

GRAVEL: rock fragments, mainly igneous, some metamorphic, maximum size 1.0 cm, average size 0.3-0.5 cm.

CLAY: gray (N4), soft, very badly disturbed.

DIATOM-BEARING CLAY: dark greenish gray (5GY 4/1), stiff, many silt layers (<1.0 cm thick). One ice-rafted basalt pebble and minor ice-rafted gravel down to Sect. 2, 69 cm. Clay composition: 76% clay mins., 15% diatoms, 9% qtz., traces fldspr., opaque mins., hematite, sponge spicules, fish remains. Silt composition: 65% qtz., 15% rock frags., 10% heavy mins., 5% fldspr., 3% diatoms.

CLAY: dark greenish gray (5GY 4/1), stiff, fine silt layers (<0.5 cm thick). Two ice-rafted basalt pebbles.

BULK X-RAY (2: 93-95)

Amorph. 56.1% Crystal. 43.9%

Percent of Crystalline Component

Quartz	24.5%	Chlorite	7.0%
K-Fldspr.	10.4%	Mont.	10.5%
Plag.	36.9%	Clinop.	0.8%
Mica	6.5%	Amphi.	3.4%

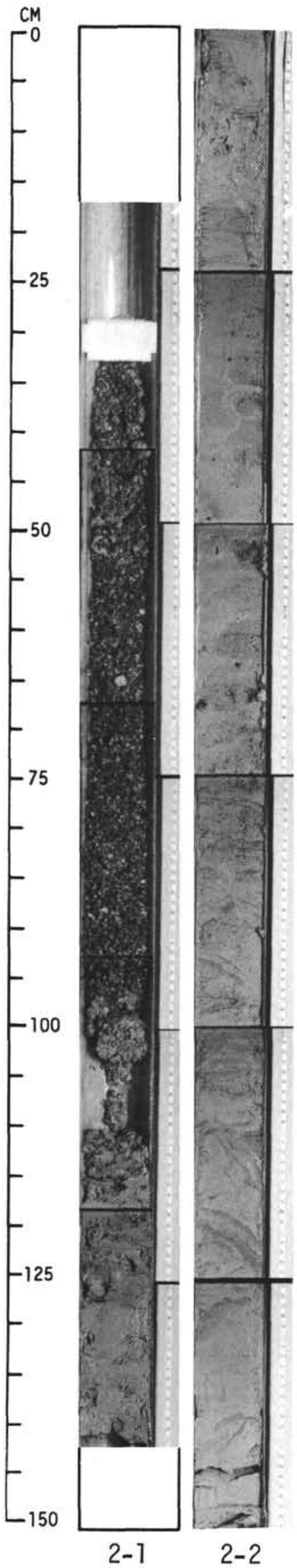
CM
0
25
50
75
100
125
150
2-1
2-2

Hole 325, Core 3 — Cored Interval: 176.5-186.0 m

AGE	ZONE	FOSSIL	ABUND.	PRES.	SECTION	METERS	LITHOLOGY	DEFORMATION	LITHO. SAMPLE
PLIOCENE	(R) Helotholus vema (D) Nitzschia interfrigidaria				0		VOID		
		D R	C F	M M	1	0.5 1.0			* * * GC
		D R	F R	M P	2				* * € x
		R D	F C	M M	2				*
		D R	C F	M M	3				* x € *
		D R	C F	M M	3				* GC
		D R	C F	M M	4				- *
	(D) Nitzschia praeinterfrigidaria	D R	C F	M M	4				x €
		D R	C F	M M	Core Catcher				*

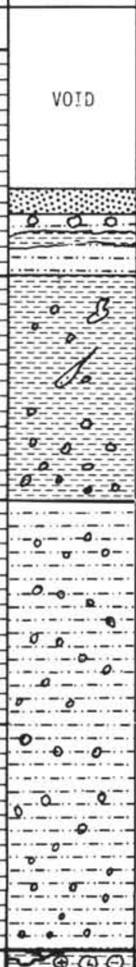

LITHOLOGIC DESCRIPTION

CLAY, CLAYEY SILT, AND SILTY CLAY

SAND: debris.

QUARTZ-CLAYEY SILT: dark greensih gray (5GY 4/1), firm, structureless. Ice-rafted pebbles at top, finer debris below. One 5 cm bed bluish (5G 4/1) clay.

CLAY AND SILTY CLAY: dark greenish gray (5GY 4/1) firm. Ice-rafted debris common to abundant. Poorly sorted silt layers (<0.5 cm thick). Clay composition: 90% clay mins., 5% qtz., 3% diatoms, 2% fldspr. Silt composition: 20-80% qtz., 7-65% clay mins., 3% fldspr., 3% heavy mins., 3% rock frags. Carbon/carbonate: 2-58 (0.3-0.2-1.0).

Section 3: dark greenish gray (5GY 4/1) firm, uniform, few layers of poorly sorted silt. Much ice-rafted debris (<0.5 cm). Carbon/carbonate: 3-65 (0.2-0.2-0.0).

Composition: 24-72% qtz., 10-65% clay mins., 2-5% fldspr., 3-5% heavy mins., 3-6% rock frags., 4-5% diatoms.

Section 4: dark greensih gray (5GY 4/1), uniform, poorly sorted. Abundant ice-rafted debris.

Composition: 60% clay mins., 25% qtz., 4% fldspr., 3% heavy mins., 6% diatoms. Carbon/carbonate: 4-132 (0.2-0.2-0.0).

DIATOM CLAY: olive gray (5GY 5/1). Ice-rafted pebbles of granite; siltstone and mudstone pebbles.

BULK X-RAY

	2: 90-92	3: 51-54	4: 121-123
Amorph.	51.2%	49.8%	49.7%
Crystal.	48.8%	50.2%	50.3%
	Percent of Crystalline Component		
Quartz	22.5%	27.1%	25.2%
K-Fldspr.	10.5%	16.5%	14.0%
Plag.	37.1%	38.8%	39.4%
Mica	7.4%	3.5%	4.9%
Chlorite	6.0%	5.0%	6.0%
Mont.	12.4%	4.9%	6.1%
Clinop.	1.1%	0.5%	0.4%
Amphi.	3.1%	4.1%	0.8%

Explanatory notes in Chapter 2

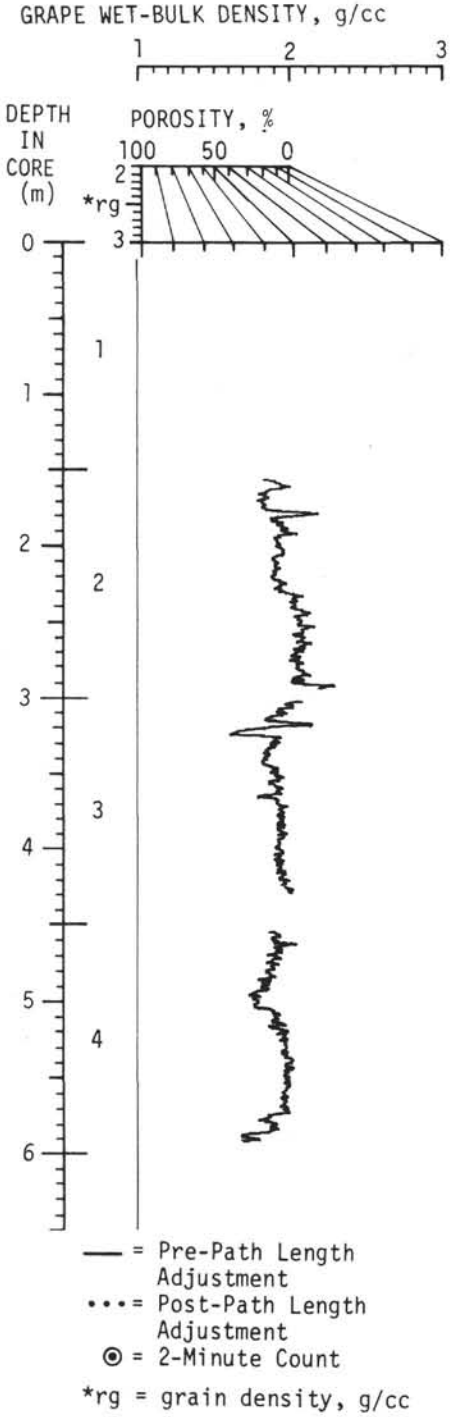
GRAPE WET-BULK DENSITY, g/cc
1
2
3
DEPTH IN CORE (m)
POROSITY, %
100
50
0
*rg
0
1
2
3
4
5
6
— = Pre-Path Length Adjustment
• • • = Post-Path Length Adjustment
⊙ = 2-Minute Count
*rg = grain density, g/cc

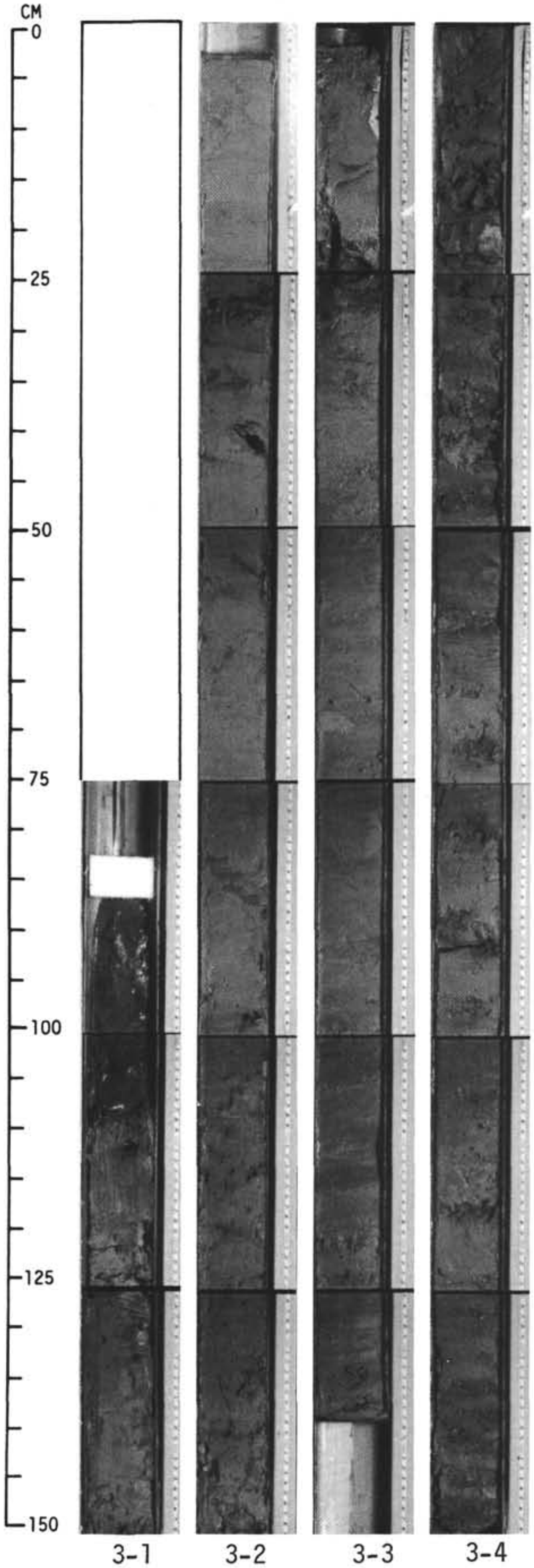
CM
0
25
50
75
100
125
150
3-1
3-2
3-3
3-4

Hole 325, Core 4 — Cored Interval: 290.5-300.0 m

AGE	ZONE	FOSSIL	ABUND.	PRES.	SECTION	LITHOLOGY
MIOCENE	(R) Theocalyptra bicornis spongothorax	R D	F F	M M	0, 1, 2, 3, Core Catcher	VOID; DRILLING BRECCIA; gravel

LITHOLOGIC DESCRIPTION

CLAYSTONE, CLAYEY SILTSTONE, AND GRAVEL

DRILLING BRECCIA WITH PIECES OF QUARTZ-CLAYEY SILTSTONE AND QUARTZ-BEARING CLAYSTONE: greenish gray (5GY 5/1), hard, poorly sorted. Sand grains probably ice-rafted. Composition: 25-49% qtz., 0-20% clay mins., 4-15% fldspr., 0-15% rock frags., 0-40% auth. carbonate, 0-25% diatom frags. Several isolated fragments of ice-rafted sandstone, siltstone and igneous and metamorphic rocks.

FINE FORMATION GRAVEL: fragments of igneous and metamorphic rocks.

Pebbles of hard diatom bearing claystone.

Ice-rafted pebbles of siltstone and mafic intrusive rock.

Hole 325, Core 5 — Cored Interval: 404.5-414.0 m

AGE	ZONE	FOSSIL	ABUND.	PRES.	SECTION	LITHOLOGY
MIOCENE	(R) Theocalyptra bicornis spongothorax	D R	— F	— M	0, 1	VOID; DRILL CUTTINGS
		R D	R F	M M	2, Core Catcher	VOID

LITHOLOGIC DESCRIPTION

CLAYSTONE AND SILTSTONE

CLAYSTONE: medium dark gray (N4), hard, some siliceous, trace fossils. Light gray (N8) silty layer at 82 cm. Some ice-rafted mafic igneous pebbles, probably from above. Composition: 88% clay mins., 7% diatoms, 5% qtz.

CALCITE-CEMENTED SILTSTONE: medium dark gray (N4). Composition: 60% authigenic carbonate, 40% qtz.

CLAYSTONE: medium dark gray (N4), trace fossils. Composition: 86% clay mins., 7% diatoms, 5% qtz., traces fldspr., heavy and opaque mins. Some ice-rafted igneous pebbles, probably from above.

DIATOM CLAYSTONE: medium dark gray (N4).

SILICIFIED CLAYSTONE: 100% authigenic silica and clay minerals.

Explanatory notes in Chapter 2

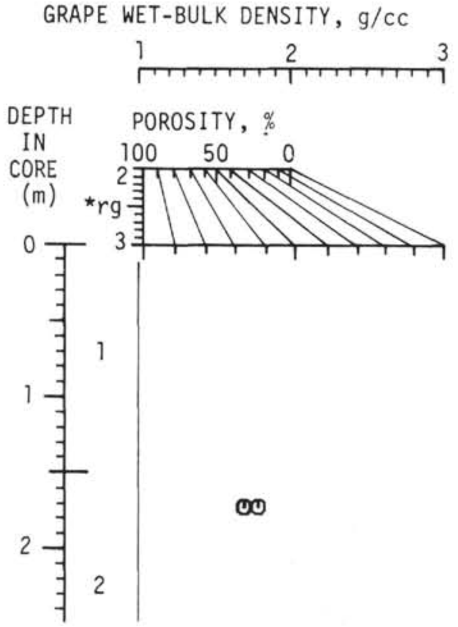

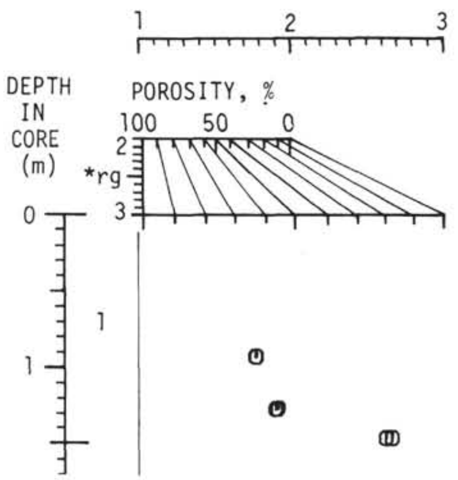

—— = Pre-Path Length Adjustment
••• = Post-Path Length Adjustment
⊙ = 2-Minute Count
*rg = grain density, g/cc

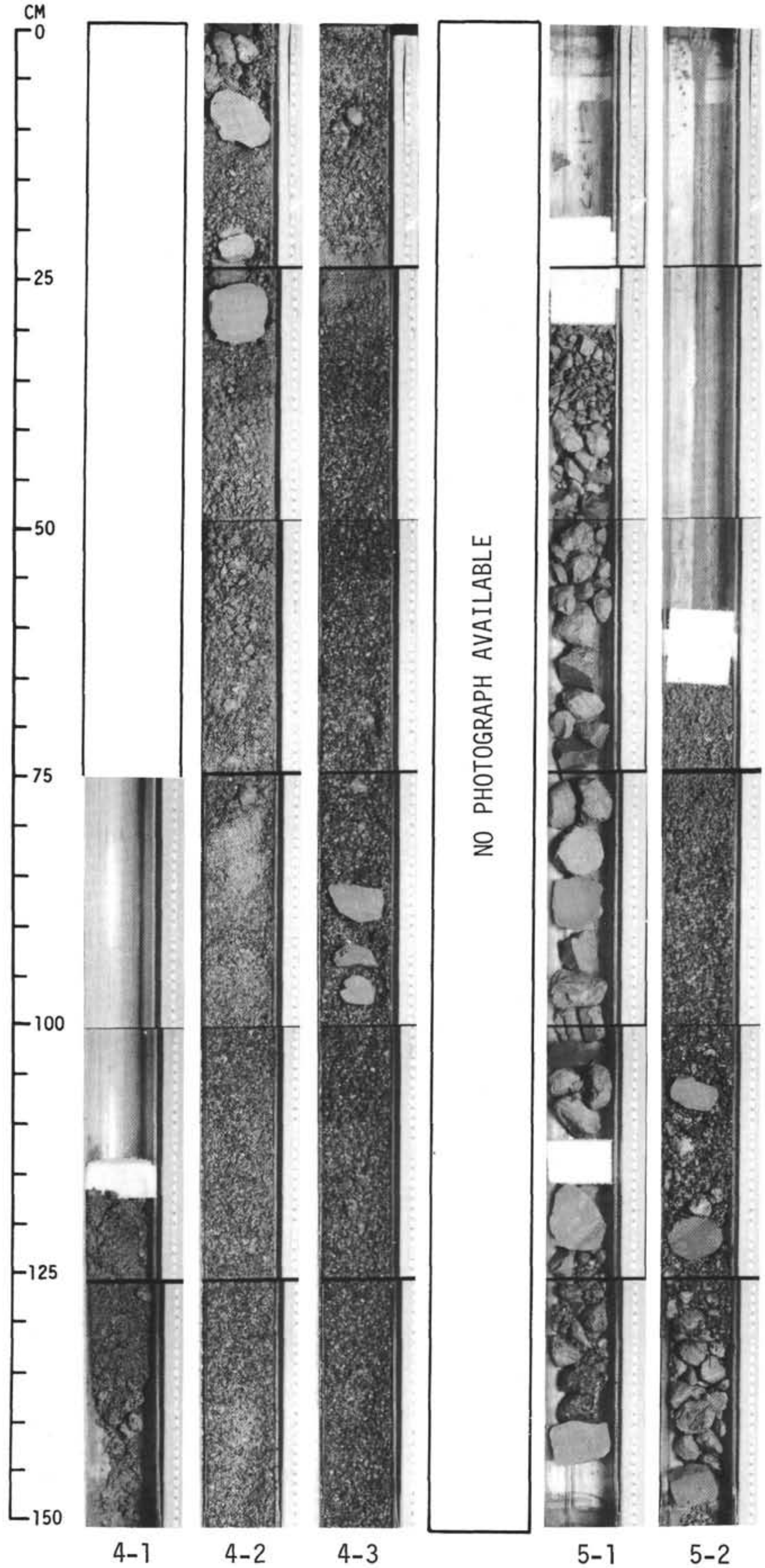

Hole 325, Core 6 Cored Interval: 480.5-490.0 m

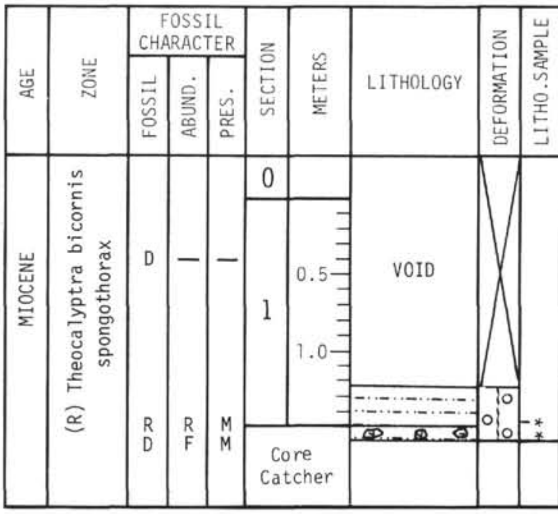

LITHOLOGIC DESCRIPTION

SILTY CLAYSTONE

SILTY CLAYSTONE: olive black (5Y 4/1). No ice-rafted detritus. Composition: 80% clay mins., 12% qtz., 7% diatoms, traces fldspr., mica, pyrite, heavy mins.

QUARTZ-SILTY CLAYSTONE: olive gray (5Y 3/1). Ice-rafted igneous pebbles.

Hole 325, Core 7 Cored Interval: 518.5-528.0 m

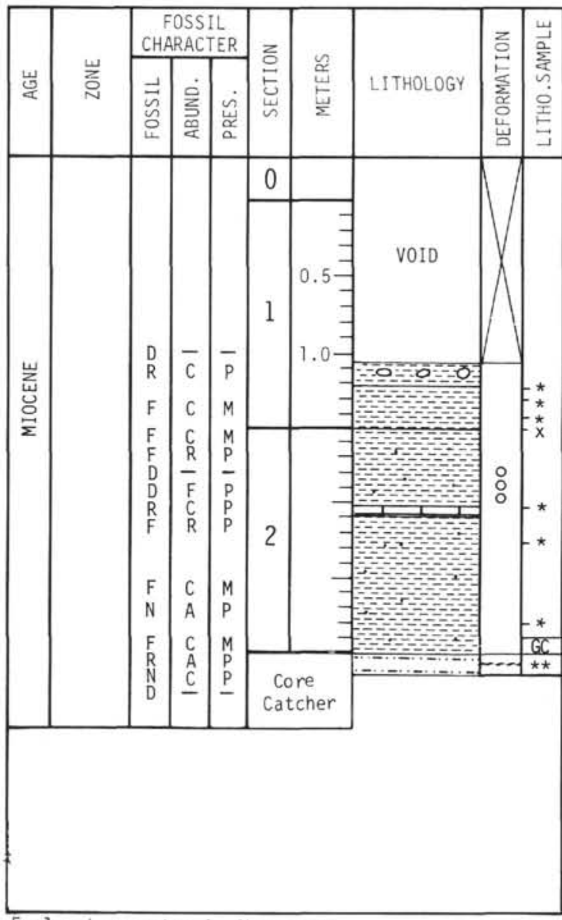

LITHOLOGIC DESCRIPTION

CLAYSTONE AND NANNOFOSSIL CHALK

CLAYSTONE: olive gray (5Y 3/1) and dark greenish gray (5G 3/1), with ice-rafted debris.

CLAYSTONE: olive black (5Y 2/1), trace fossils.

CLAYSTONE: medium dark gray (N4), trace fossils, burrows, forams, nannos, ice-rafted sand grains.

NANNOFOSSIL CHALK: light gray (N7), >95% nannos., (52% $CaCO_3$).

CLAYSTONE: medium dark gray (N4), locally silicified, trace fossils, ice-rafted sand grains. Composition: 95% clay mins., 4% qtz., (5% $CaCO_3$ at 137 cm).

SILTY CLAYSTONE: medium dark gray (N4), some with siliceous cement.

BULK X-RAY (2: 0-2)

Amorph. 45.6% Crystal. 54.4%

Percent of Crystalline Component

Quartz	13.9%	Chlorite	3.0%
Crist.	28.2%	Mont.	9.5%
K-Fldspr.	15.3%	Clinop.	1.4%
Plag.	26.0%	Amphi.	0.8%
Mica	1.9%		

Explanatory notes in Chapter 2

GRAPE WET-BULK DENSITY, g/cc

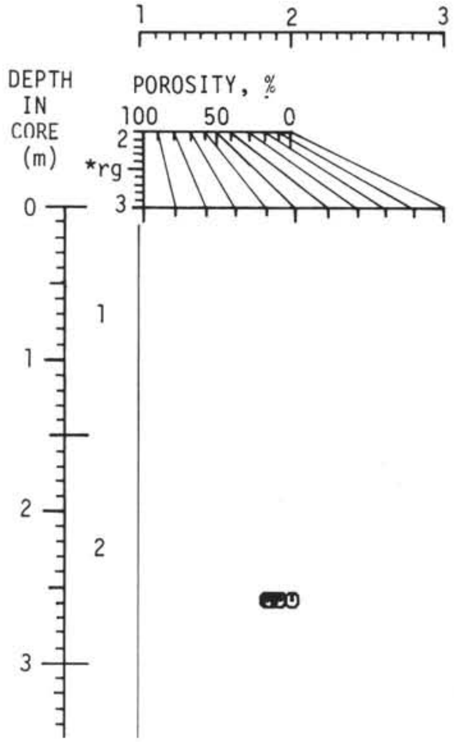

— = Pre-Path Length Adjustment
••• = Post-Path Length Adjustment
⊙ = 2-Minute Count
*rg = grain density, g/cc

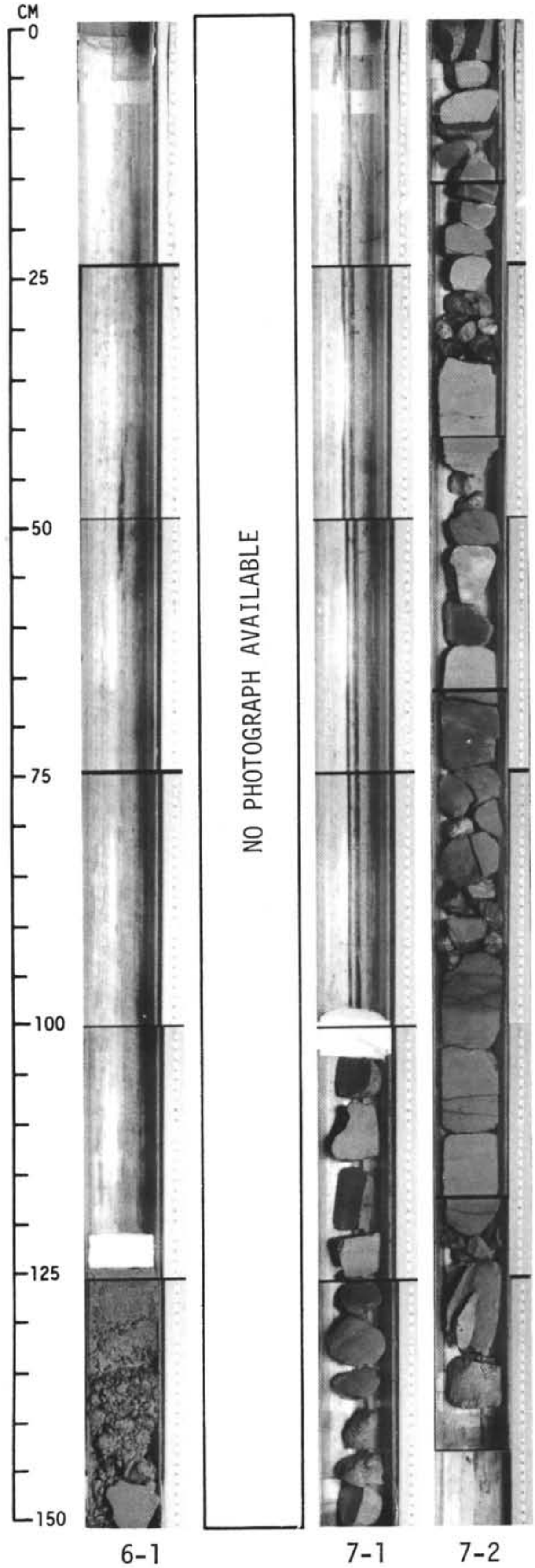

Hole 325, Core 8 Cored Interval 612.5-622.0 m

AGE	ZONE	FOSSIL	ABUND.	PRES.	SECTION	METERS	LITHOLOGY	DEFORMATION	LITHO.SAMPLE
EARLY TO MIDDLE MIOCENE	(Barren)				0		VOID		
		R F D	A R —	P P —	1	0.5			*
		R	A	P		1.0			*
		D	—	—					*
		F	C	M					X
		D	—	—	2				€ *
		N	A	P					*
		R D F R D	C C F —	P M P —					X * GC
					3				* € * X
		D F R N F D	— F C A F —	— M P P M —	Core Catcher				**

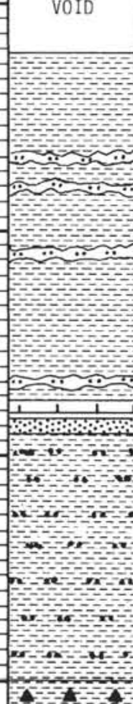

CLAYSTONE WITH NANNOFOSSIL CHALK AND SANDSTONE BEDS

CLAYSTONE: olive black (5Y 2/1), with trace fossils. Thin silt and sand beds, some with clay laminae. Pyrite in one bed. One bed shows flame structure and forset beds.

Composition: 76% clay mins., 11% qtz., 10% recrystallized silica, 1% heavy mins., traces fldspr., opaque mins., zeolites, diatoms. (2% $CaCO_3$ at 97 cm, Sect. 2).

Carbon/carbonate: 2-35 (0.3-0.2-0.0).

NANNOFOSSIL CHALK: medium dark gray (N4), with silt and trace fossils. (31% $CaCO_3$).

SANDSTONE: medium dark gray (N4), qtz., rock frags. up to 2 mm diam.

CLAYSTONE: medium dark gray (N4) with light gray silt laminae. Trace fossils at top.
Carbon/carbonate: 3-142 (0.3-0.3-0.0).

BULK X-RAY

	1: 147-149	2: 112-113	3: 130-133
Amorph.	47.6%	41.1%	38.8%
Crystal.	52.4%	58.9%	61.2%
Percent of Crystalline Component			
Calcite	4.4%	13.7%	-
Quartz	14.6%	12.8%	9.5%
Crist.	21.6%	18.3%	25.3%
K-Fldspr.	7.2%	16.9%	6.3%
Plag.	22.8%	18.9%	12.0%
Mica	4.0%	5.1%	35.0%
Chlorite	4.1%	2.0%	1.4%
Mont.	18.6%	10.2%	6.0%
Trid.	-	-	2.0%
Clinop.	1.8%	1.5%	2.3%
Amphi.	0.8%	0.7%	0.2%

CLAYSTONE: greenish black (5G 2/2), silicified, some silt, chert.

Explanatory notes in Chapter 2

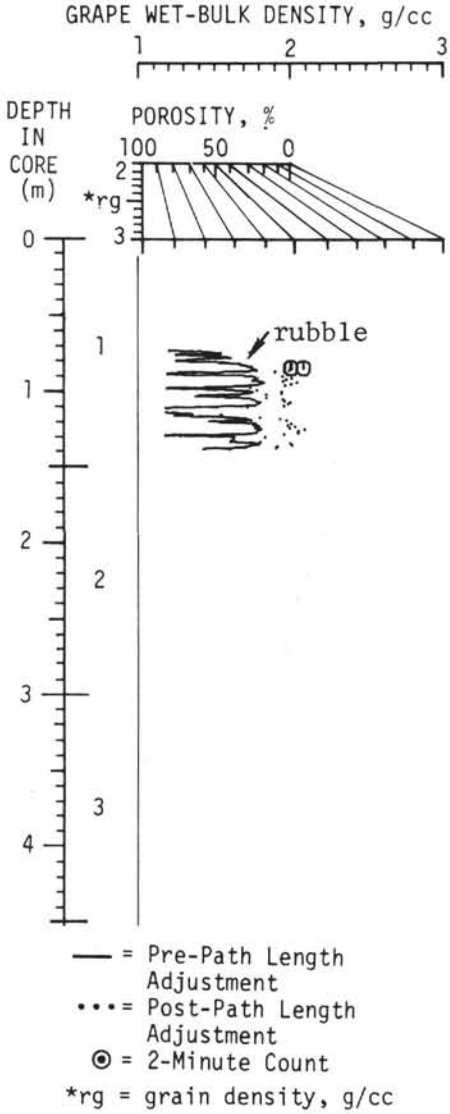
GRAPE WET-BULK DENSITY, g/cc
1
2
3
DEPTH IN CORE (m)
POROSITY, %
100
50
0
*rg
rubble
0
1
2
3
4
1
2
3
— = Pre-Path Length Adjustment
•••= Post-Path Length Adjustment
⊙ = 2-Minute Count
*rg = grain density, g/cc

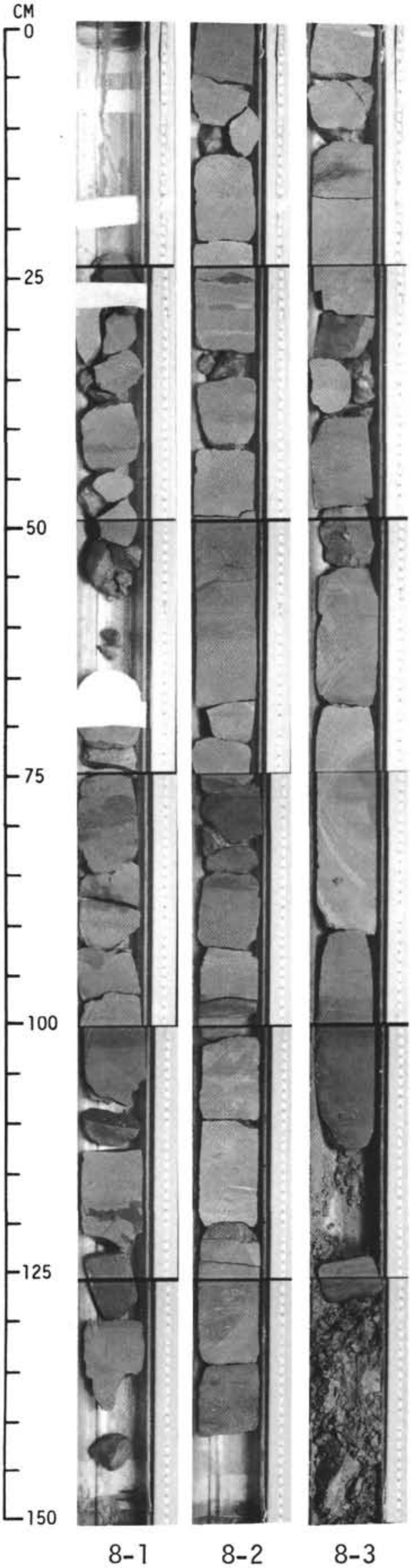
CM
0
25
50
75
100
125
150
8-1
8-2
8-3

Hole 325, Core 9 Cored Interval: 641.0-650.5 m

AGE	ZONE	FOSSIL	ABUND.	PRES.	SECTION	METERS	LITHOLOGY	DEFORMATION	LITHO. SAMPLE	LITHOLOGIC DESCRIPTION
EARLY TO MIDDLE MIOCENE	(Barren)				0					SANDSTONE, SILTSTONE, AND CLAYSTONE
					1	0.5, 1.0	VOID			
		D R F R D	— C R R —	— P C P —					* * GC *	SILTY CLAYSTONE: dark gray (N3) with light gray (N7) silt laminae. Siltstones poorly sorted with up to 20% rock frags. SANDSTONE: dark gray (N3), dries to light gray (N7), 19% feldspar, 17% rock frags. Small fault present.
		F R D D R D D	A C — C — —	M P — P — —	2				* € X * X	CLAYSTONE: dark gray (N3). INTERBEDDED SANDSTONE, SILTSTONE AND CLAYSTONE: dark gray (N3). Some beds show fine light gray (N7) siltstone laminations. No apparent size grading. Carbon/carbonate: 9-104 (0.2-0.2-0.0). SANDSTONE WITH SILTSTONE AND CLAYSTONE: medium dark gray (N4-N3), many laminations. Composition: 34% clay mins., 30% rock frags., 17% qtz., 10% fldspr.
		D R F D R D F	— C A — C F A	— P M — P P M	3				* X € *	CLAYSTONE WITH SILTSTONE AND SANDSTONE: dark gray (N3). Silt laminae undisturbed. Composition: 90% clay mins., 5% qtz., 2% fldspr. SANDSTONE AND SILTSTONE WITH CLAYSTONE: dark gray (N3) with light gray (N7) laminae, mainly undisturbed. Carbon/carbonate: 3-95 (0.2-0.1-0.0).
		R F D	A C F	P M D	Core Catcher					CLAYSTONE: gray (N3).

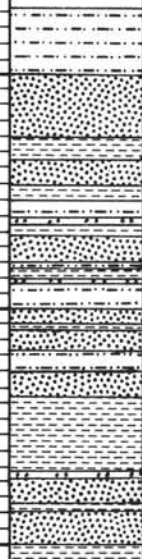

BULK X-RAY

	2: 106-110	3: 92-95
Amorph.	31.3%	42.0%
Crystal.	68.7%	58.0%
Percent of Crystalline Component		
Quartz	23.8%	15.2%
K-Fldspr.	17.6%	15.8%
Plag.	34.4%	28.1%
Mica	1.5%	8.0%
Chlorite	1.3%	4.7%
Mont.	7.2%	22.5%
Clinop.	13.6%	4.4%
Amphi.	0.6%	1.3%

Explanatory notes in Chapter 2

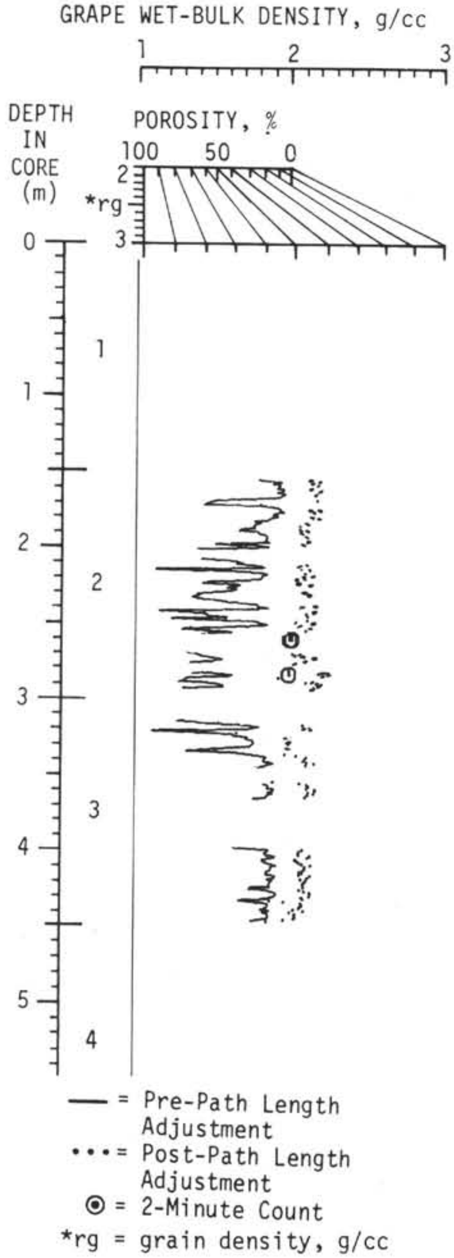
GRAPE WET-BULK DENSITY, g/cc
1
2
3
DEPTH
IN
CORE
(m)
POROSITY, %
100
50
0
*rg
2
3
0
1
2
3
4
5
1
2
3
4
—— = Pre-Path Length Adjustment
• • • = Post-Path Length Adjustment
⊙ = 2-Minute Count
*rg = grain density, g/cc

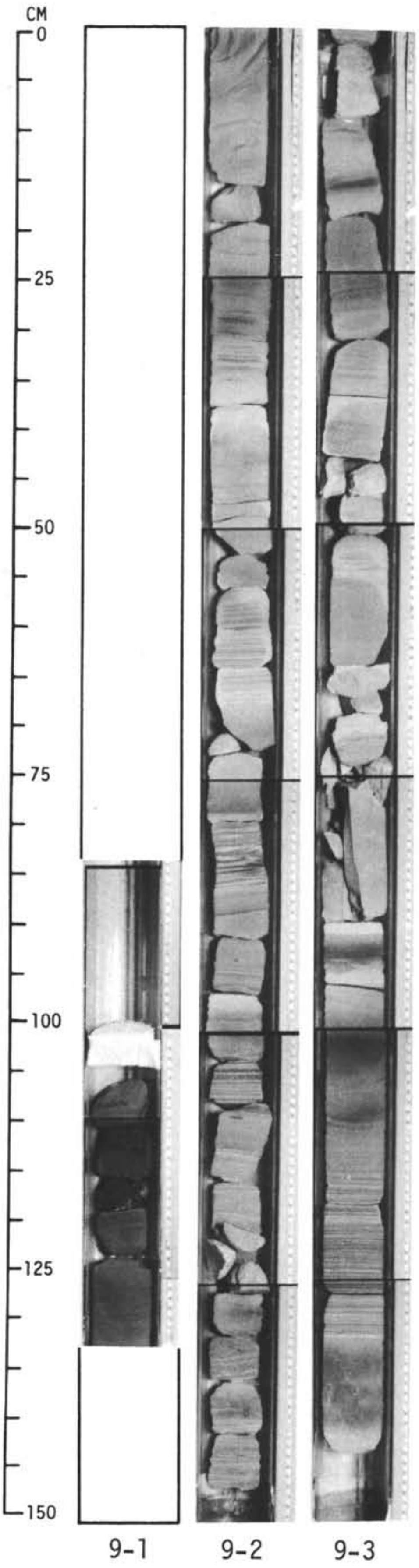
CM
0
25
50
75
100
125
150
9-1
9-2
9-3

Hole 325, Core 10 — Cored Interval: 708.5-718.0 m

AGE	ZONE	FOSSIL	ABUND.	PRES.	SECTION	METERS	LITHOLOGY	DEFORMATION	LITHO.SAMPLE
EARLY MIOCENE	(F) *Zealandica incognita*				0		VOID		
		D R F	C C	P M	1	0.5, 1.0			*, *, *
		D R F	C C	P M	2				GC, X €, *, *
		D R F	C C	P M	3				*, *, X,€, *, *
		D R F	C C	P M	Core Catcher				*, *

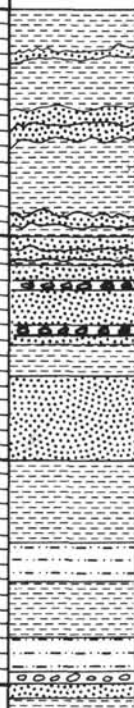

LITHOLOGIC DESCRIPTION

CLAYSTONE, SANDSTONE, AND CONGLOMERATE

CLAYSTONE: greenish gray (5GY 5/1) and greenish black (5G 2/1), with poorly sorted sandstone beds. Contains 95% clay mins. Sandstone composition: 43% rock frags., 20% fldspr., 18% qtz., 12% clay mins.

SANDSTONE WITH CLAYSTONE AND CONGLOMERATE: medium dark gray (N4). Conglomerate clasts are clay with preferential orientation parallel to bedding. Some claystone dark greenish gray (5G 5/1). Sandstone composition: 40% rock frags., 25% fldspr., 20% qtz., 12% heavy mins. Claystone composition: 95% clay mins., 2% qtz., 1% opaque mins., 1% heavy mins. Carbon/carbonate: 2-50 (0.1-0.1-0.0).

SILTY AND SANDY CLAYSTONE: dark gray (N3) with light gray (N7) silty layers.

Carbon/carbonate: 3-71 (0.2-0.2-0.0).

CONGLOMERATE: well rounded clasts of clay, no preferential orientation, carbonate matrix, 49% $CaCO_3$.

SANDSTONE: medium dark gray (N4), fine- to coarse-grained, well sorted, contains qtz., rock fragments, fldspr., glauconite, with calcareous cement.

CLAYSTONE: dark gray (N3), 89% clay mins. with recrystallized silica.

BULK X-RAY

	2: 46-48	3: 71-73
Amorph.	11.8%	29.0%
Crystal.	88.2%	71.0%
Percent of Crystalline Component		
Quartz	6.6%	22.7%
K-Fldspr.	14.2%	19.7%
Plag.	22.4%	32.4%
Mica	-	2.9%
Chlorite	0.7%	1.7%
Mont.	51.9%	5.4%
Clinop.	3.7%	14.7%
Amphi.	0.5%	0.6%

Explanatory notes in Chapter 2

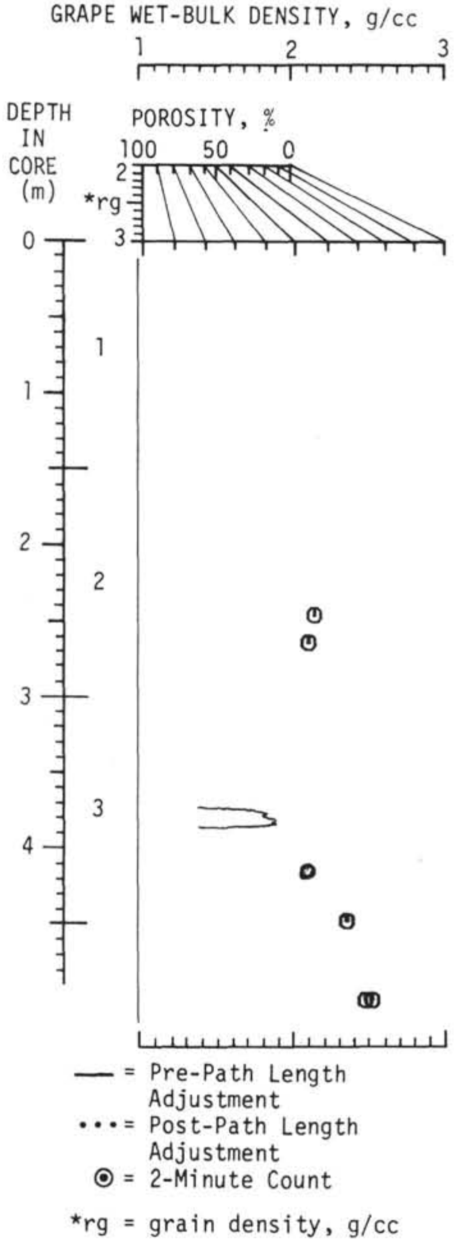
GRAPE WET-BULK DENSITY, g/cc
1
2
3
DEPTH IN CORE (m)
POROSITY, %
100
50
0
*rg
0
1
2
3
4
—— = Pre-Path Length Adjustment
• • • = Post-Path Length Adjustment
⊙ = 2-Minute Count
*rg = grain density, g/cc

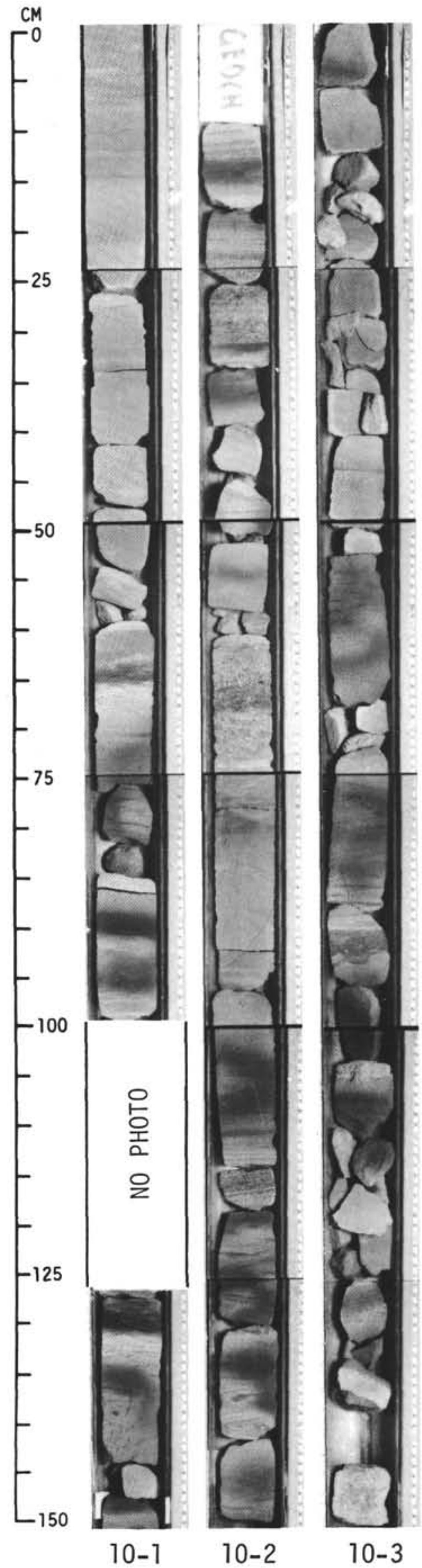
CM
0
25
50
75
100
125
150
NO PHOTO
10-1
10-2
10-3

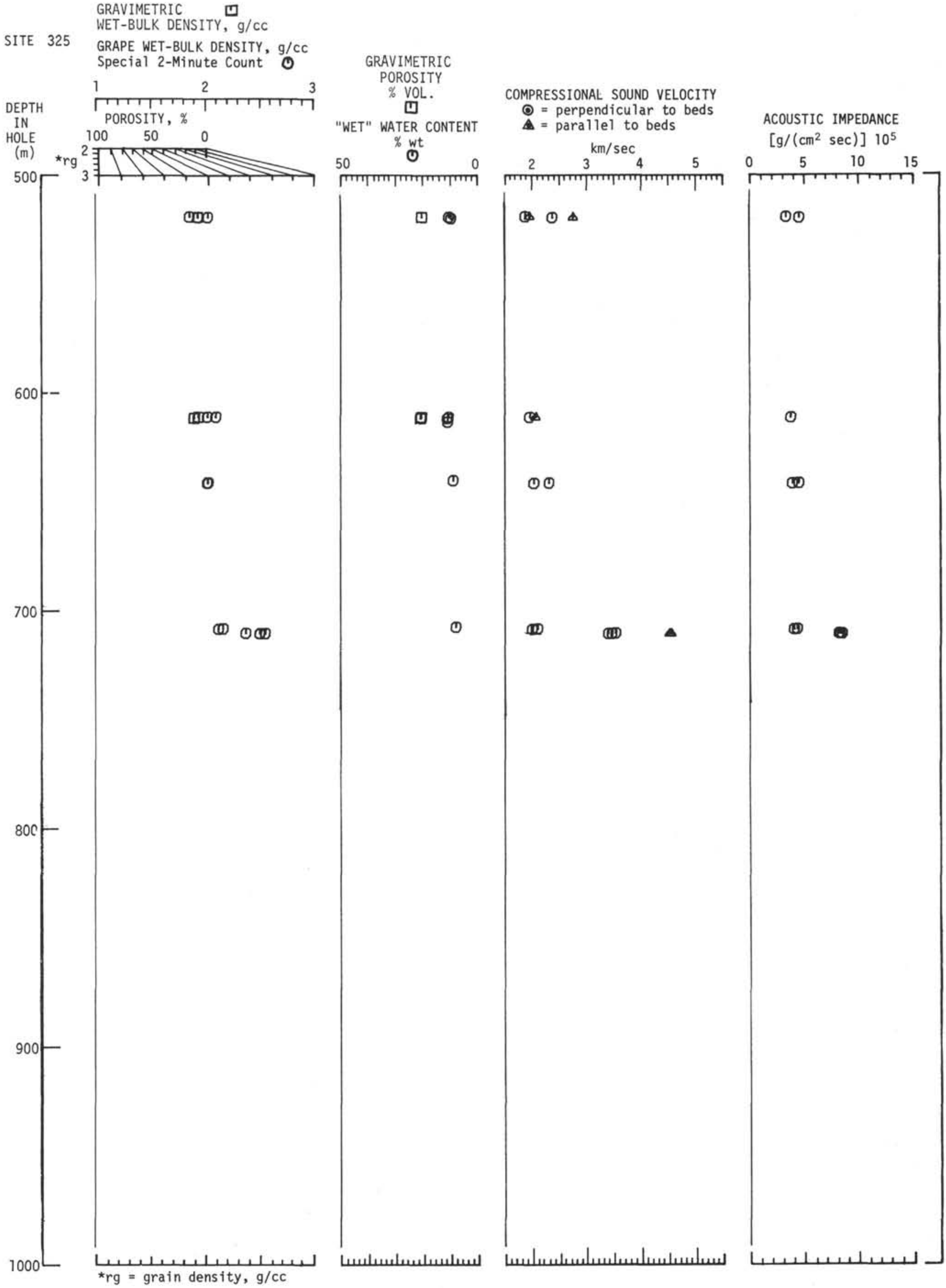
SITE 325
GRAVIMETRIC WET-BULK DENSITY, g/cc
GRAPE WET-BULK DENSITY, g/cc
Special 2-Minute Count
1 2 3
POROSITY, %
100 50 0
*rg
DEPTH IN HOLE (m)
500
600
700
800
900
1000
*rg = grain density, g/cc
GRAVIMETRIC POROSITY % VOL.
"WET" WATER CONTENT % wt
50 0
COMPRESSIONAL SOUND VELOCITY
= perpendicular to beds
= parallel to beds
km/sec
2 3 4 5
ACOUSTIC IMPEDANCE
[g/(cm² sec)] 10⁵
0 5 10 15

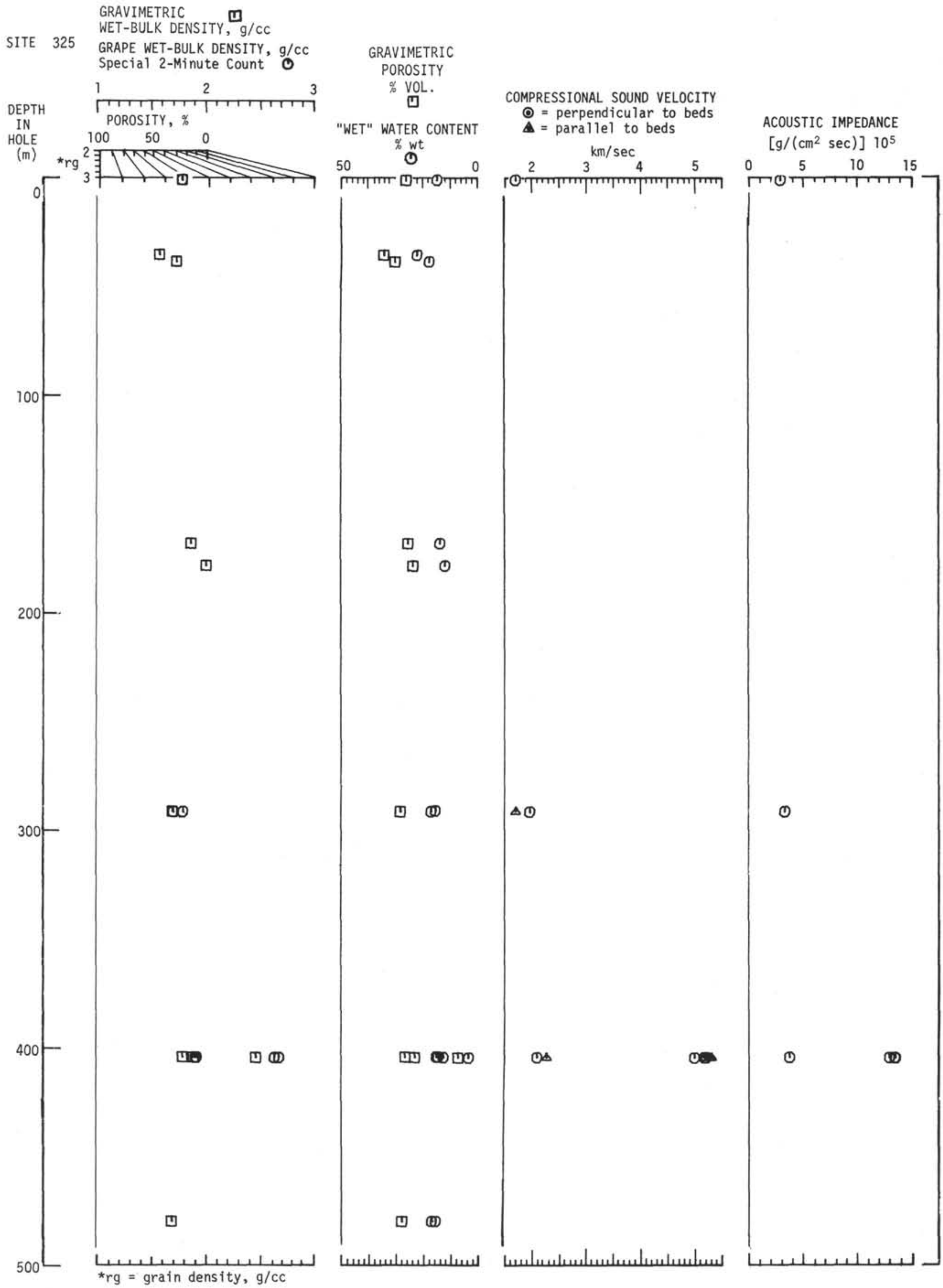
SITE 325
GRAVIMETRIC WET-BULK DENSITY, g/cc
GRAPE WET-BULK DENSITY, g/cc
Special 2-Minute Count
1
2
3
POROSITY, %
100
50
0
*rg
2
3
DEPTH IN HOLE (m)
0
100
200
300
400
500
*rg = grain density, g/cc
GRAVIMETRIC POROSITY % VOL.
"WET" WATER CONTENT % wt
50
0
COMPRESSIONAL SOUND VELOCITY
= perpendicular to beds
= parallel to beds
km/sec
2
3
4
5
ACOUSTIC IMPEDANCE
[g/(cm2 sec)] 105
0
5
10
15